# Current status and technical challenges of electrolytes in zinc–air batteries: An in-depth Review

Soraya Hosseini.[1], Salman Masoudi Soltani.[2], Yuan-Yao Li [1,3,*]

[1]Department of Chemical Engineering, National Chung Cheng University, Min-Hsiung, Chiayi 62102, Taiwan

[2]Department of Chemical Engineering, College of Engineering, Design and Physical Sciences, Brunel University London, Uxbridge UB8 3PH, United Kingdom

[3]Advanced Institute of Manufacturing with High-Tech Innovations, National Chung Cheng University, Min-Hsiung, Chia-Yi 62102, Taiwan.

* Corresponding author: E-mail: chmyyl@ccu.edu.tw

## Abstract

In the past few years, there has been a growing level of interest in the research and development of energy storage systems such as batteries. This is a direct consequence of the soaring rise in global energy demand across various commercial and industrial sectors. Lithium ion batteries have set out a feasible horizon for widespread deployment as small-scale energy storage devices due to their high efficiency and cyclability. However, the availability and cost of lithium have limited the commercial deployment of large-scale systems. On the other hand, zinc-air batteries have demonstrated comparable efficiencies and have been reported to be suitable replacements for lithium batteries in large-scale applications. Nevertheless, more research has been undertaken to address the issues associated with the cycling processes of these batteries. Secondary zinc-air batteries are yet to be commercially proven feasible due to the low charge/discharge cycle life of electrodes. The main problems of secondary alkaline zinc–air batteries are dendritic growth resulting in an alternation of morphology and structure, self-dissolution and the consequent occurrence of hydrogen evolution reactions. However, by and large, inefficient electrolytes are the main culprits responsible for the reduced performance of zinc-air batteries. Therefore, a comprehensive review of current advancements in the development of suitable electrolytes to promote zinc-air batteries towards commercial application will provide a perspective for future rechargeable zinc-air batteries. In this in-depth review, the effects of the types of electrolytes and their properties on the electrochemical

performance of Zn anode have been discussed. A demonstration of the current research status and challenges set upon the large-scale deployment of zinc-air batteries will facilitate the educated steering of future research directions in this critically important realm.

**Keywords:** zinc-air batteries; rechargeable; liquid electrolyte; non-aqueous electrolytes

## 1. Introduction

There has been an increasing demand for clean and renewable energy due to the rise in the energy consumption in modern societies and the continual birth of advanced technologies. There have been great efforts to improve the existing and/or devise new advanced energy storage systems. With the inherently intermittent nature of wind and solar energies, there has been a growing research interest in the development of various types of batteries as energy storage devices. Such research; however, needs to consider the abundancy of resources, cost, energy density, safety aspects and cycle life for feasible large-scale implementation [1]. Despite the great success of lithium-ion batteries in the current market, the limited global resources of lithium, as well as the corresponding high costs, both restrict their practical and industrial applications [2]. Therefore, alternative low-cost and abundantly-available elements must be identified, researched and developed for commercially-feasible applications [3].

Unlike lithium, zinc is abundant, lighter, more stable, inexpensive, safer and environmentally friendly. It also demonstrates a relatively high specific capacity (*i.e.* energy density). High theoretical specific energy density of zinc-ion batteries (*i.e.* five times higher than their lithium-ion counterparts), plus easy re-generation from aqueous electrolyte *via* electrodepositing method, well justifies their use as secondary batteries. Theoretical specific capacities and specific energies of metal-air batteries are given in Fig. 1.
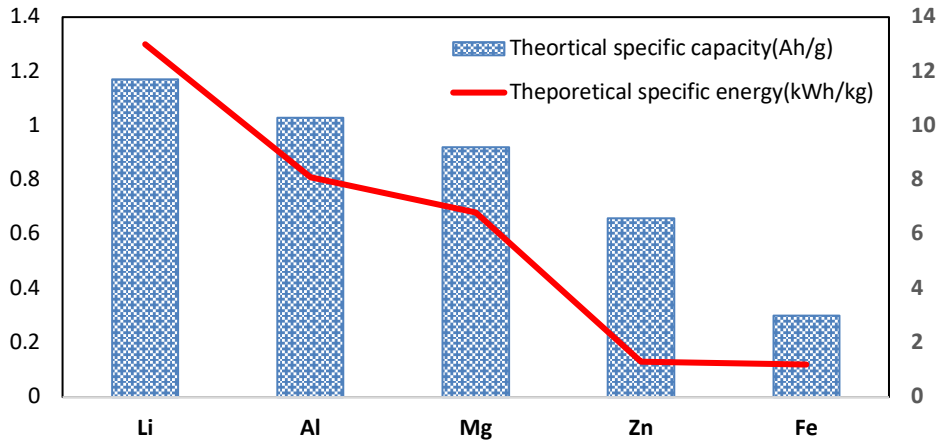
**Fig. 1.** Characteristics of metal-air batteries [4]

In general, metal-air batteries have demonstrated the potential for being further developed into potentially preferential technologies in energy storage; they present high energy densities, are reliant on the freely-available atmospheric oxygen to work and are lightweight to build, hence a significant reduction in the costs. Although Al-air (8.1kWh/kg) and Mg-air (6.8 1kWh/kg) batteries demonstrate high theoretical energy densities, Al and Mg are not rechargeable due to corrosion, short shelf life as well as cell irreversibility. As a consequence, more research has been centred on Li- and Zn-air batteries. The growing interest in Li-air batteries directly stems from the very high theoretical energy density (11.680 kWh/kg) of these devices: approximately 30 times higher than that of the Li-ion batteries and 11 times the Zn-air batteries' (1.084 kWh/kg). Lithium, with a theoretical specific capacity of 3860 mAh/g and a low potential of -3.040 V, is known to be the most effective anode compared to other electrodes [5-6]. Compared to Zn batteries, the key limiting factors in widespread deployment of Li batteries are the scarcity of resources, high production costs and stringent safety considerations. On the top of that, lithium is very sensitive to humidity and the presence of oxygen, hence operability limitations under controlled environments.

The cost of the electrode's raw material per kWh is estimated at $1.00 and $17 for Zn- and Li-ion batteries, respectively [7]. In 1994, approximately 6,819,000 tonnes of zinc were mined worldwide with 140 m tonnes in reserves. In 2005, the corresponding figures rose to 10m and 220m tonnes, respectively [8]. Although, the primary zinc-air batteries were first commercialized in the 1930s, a number of limiting barriers have been identified in the application of secondary zinc-air batteries. Consequently, many researches have been striving to overcome such issues. These problems can be classified into four main areas of these batteries: zinc anode and cathode electrodes, the electrolyte and the separator. Two types of degradation in both electrodes take place in zinc-air batteries: the morphological changes of the Zn anode (cycling) and the degradation of the cathode materials (charging). However, most attempts continue to be focused on commercialising secondary zinc-air batteries, targeting a range of applications. On a commercial scale, zinc-air batteries have been used in hearing-aid devices [2,9]. The main reactions taking place in a primary zinc-air battery comprise: I) Zn dissolution, II) ZnO precipitation, III) Oxygen absorption into the electrolyte, IV) Oxygen reduction, V) Dissolution of atmospheric carbon dioxide and carbonate formation [10] (Fig. 2).
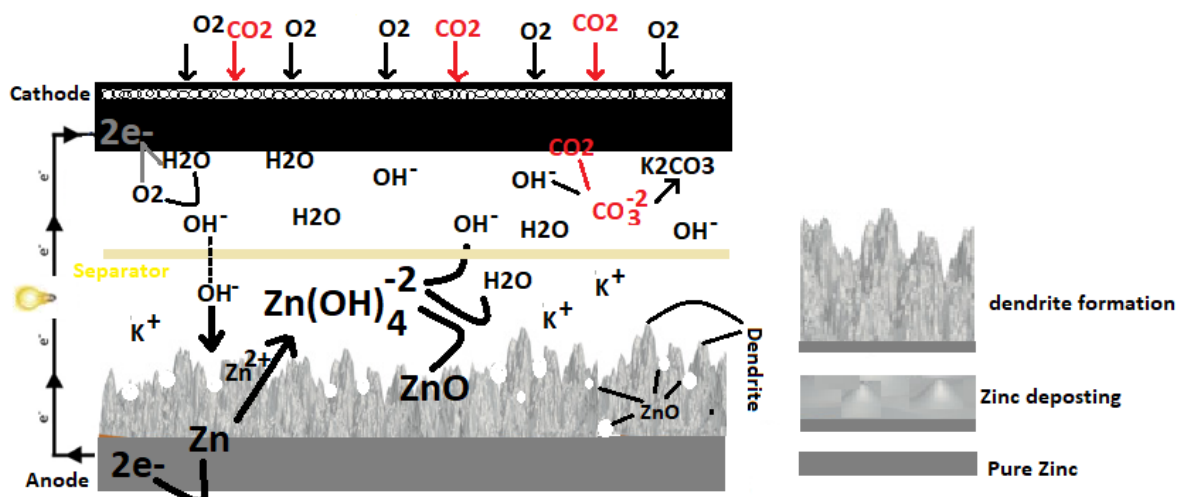


**Fig. 2.** reactions in primary zinc-air batteries

Zinc-air batteries present several drawbacks, mainly originating from the use of aqueous electrolytes - ultimately adversely impacting the performance of zinc electrodes [11-12]. Electrically rechargeable zinc-air batteries are associated with dendrite formation, hydrogen evolution reaction (HER), deformation and limited cycle lives. However, the limited cycle life and dendrite formation are typically addressed by altering the system in the mechanically rechargeable zinc-air batteries. While the undesirable humidity in the ambient air can lead to flooding in the air electrode, dry air, on the other hand, could negatively accelerate electrolyte evaporation [13]. A schematic based on main issues and the role of electrolytes for improving the performance shown in Schematic 1.
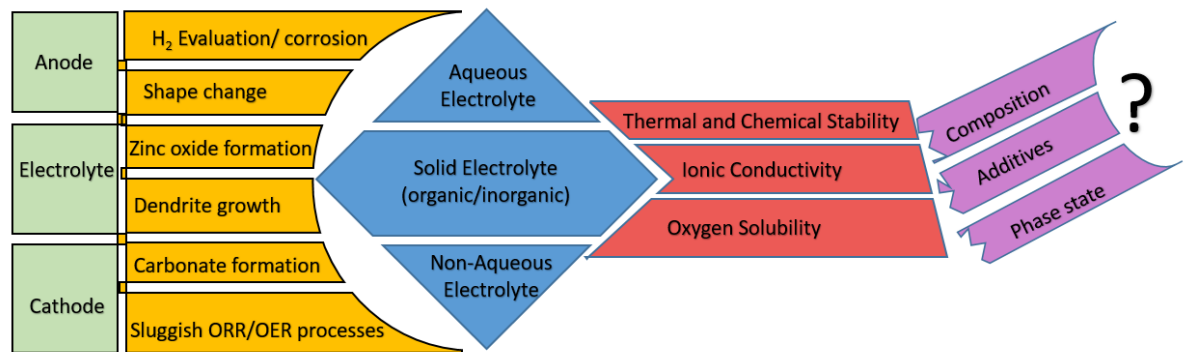


Schematic 1. Summarization of evaluation parameters for zinc-air batteries

## 2. Main Challenges in the Applications of ZABs

### 2.1 Dendrite formation

There has been significant research to effectively tackle dendrite growth (charge), deformation (cycling), passivation layer ZnO (discharge) and hydrogen evolution (cycling). Moreover, the self-discharge, an undesirable side reaction, takes place in an aqueous electrolyte solution, leading to a drop in the battery's performance (*i.e.* 2% a year) and efficiency. It is generally recommended to store these batteries at lower temperatures to slow down this reaction [3,14]:

$$Zn + H_2O \rightarrow H_2 \uparrow + ZnO \tag{1}$$

Needle-like metallic protrusions are resulted from zinc dendrites that cause short-circuit between anode and cathode. Dendrite formation (a function of overpotential) is initiated as a result of a difference in overpotential along the surface. It is then deposited around screw dislocations with a narrow range of overpotentials, leading to raised edges on the zinc electrode surface. These locations show a higher overpotential compared to the lattice structure of the electrode. The higher diffusion rates of ions from the electrolyte onto the three-dimensional (3D) raised locations (*i.e.* screw dislocations as shown Fig. 3(a), causes an accelerated rate of reduction compared to the surrounding areas on the electrode. Indeed, zinc dendrites accelerate growth at critical overpotentials, while several parameters e.g. zincate concentration, local current density and temperature have also affect the initiation of the growth [15]. Several mechanisms have been proposed to describe dendrite formation during the dissolution-electrodeposition processes. It is commonly believed that micro-scale coarse elements on the Zn surface are formed and lead to the enhancement of 3D diffusional transport of the Zn ions (during Zn electrodeposition), while mitigating the diffusion limitations. Thus, deposition rates are raised significantly at the tips of these coarse elements, ultimately resulting in dendrite formation [16]. Figure 3(c) shows the much higher energy barrier for zinc nucleation compared to zinc growth on the nucleus. The overpotential of zinc nucleation is much larger than that of the zinc growth on the nucleus (Fig. 3(d)). Many researchers have suggested the formation of the initial zinc nucleus as support as zincate ions have a tendency to deposit on these supports rather than forming a new nucleus. The movement of zinc ions towards a nucleus occur owing to concentration gradients and the driving forces resulting from the electric fields. The distributions of zinc ions and the electric field at the interface of electrode/electrolytes is important in the understanding of zinc deposition. Dendrite growth is faster due to the uneven distribution of electric field around the edges/corners of current collectors. Also, the variable

6

transfer rates of zinc ions at the interface and the bulk solution may lead to considerable concentration polarization. Zincates prefer to migrate to the tips of the bumps on the electrode's surface, resulting in surface inhomogeneity and hence, facilitating dendrite formation. This inhomogeneity is caused by the free diffusion of zinc ions on the electrode's surface. Due to the high surface energy of small nucleus, the particles thermodynamically tend to aggregate into larger particles, resulting in the development of a tree-like form [17,18]. The mechanism of zinc deposition affects dendrite formation. The diffusion-controlled approach is known to be the most effective to control dendrite growth, whilst the activation-controlled pathway may accelerate the generation of dendrites. Accordingly, structured anodes, electrolyte modification, introduction of new electrolytes, ion transfer control and electric field regulation have been proposed by different researches in the literature [18].
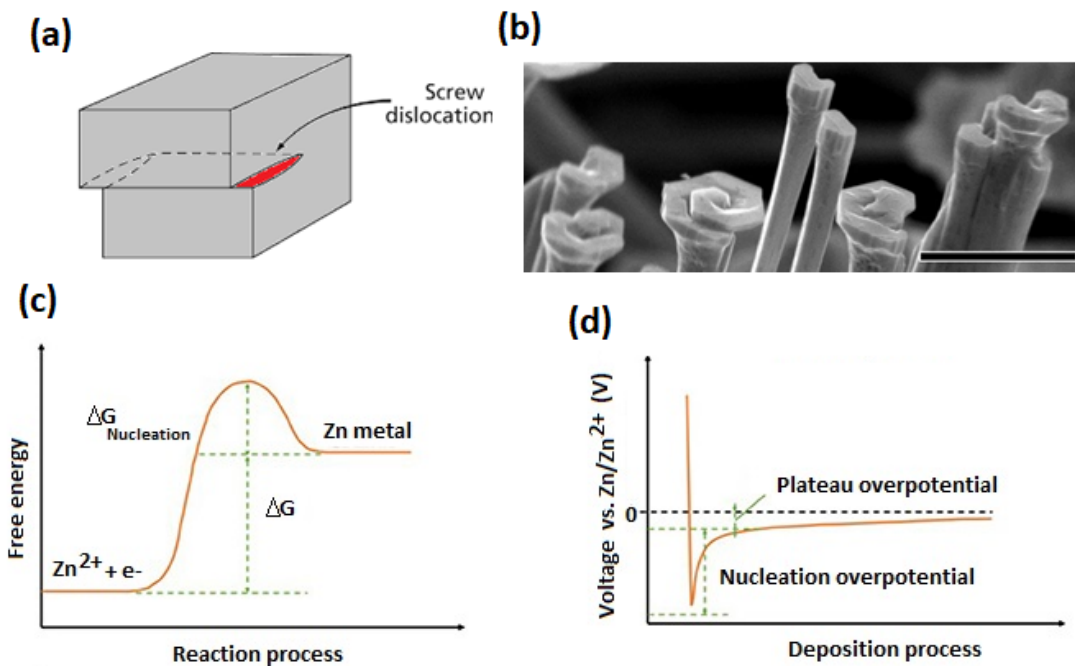


**Fig. 3.** (a) a schematic of screw dislocations crystals and, (b) flower growth ( ZnO ) [19], (c) the energy barrier for zinc nucleation and growth processes[18], (d) overpotential of zinc nucleation and growth processes,Reprinted with permission from [17], Copyright (2017) American Chemical Society

Various morphologies such as mossy, dendritic, filamentous, layer-like and boulder have been observed depending on electrolyte composition (zincate ions) and the current density (Fig. 4) [20,21]. Riede et al. (2018) studied the influence of zinc ion concentration on anode surface and the crystallization of zinc ions on the charging behaviour of a zinc-air battery. The results suggested that critical surface concentrations played a key role in forming dendritic zinc crystals [22].
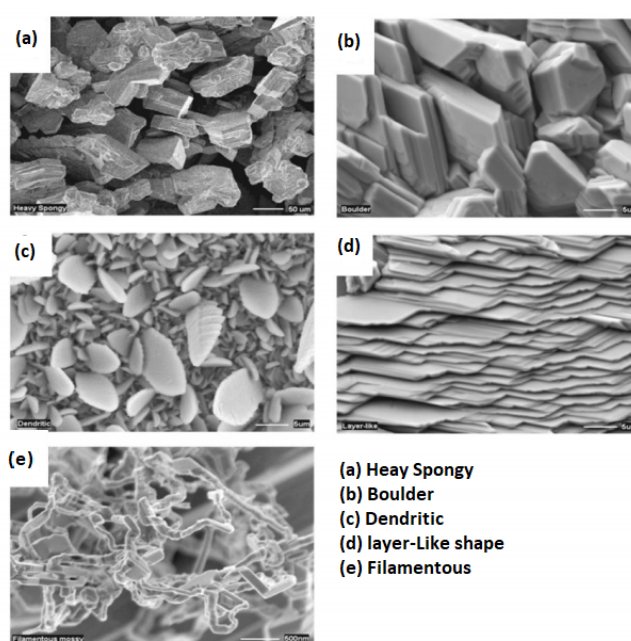


**Fig. 4.** scanning electron microscope (SEM) images of various Zn deposit morphologies, Reproduced with permission from Ref. [20] Copyright 2006 from Electrochemical Society

In order to understand the mechanism of Zn dendrite, various methods have been investigated to establish a concept for dendrite formation e.g. synchrotron x-ray tomography, advanced operando techniques, *ex-situ* XRD and phase-field model simulation. Yufit et al. (2014) reported the application of synchrotron x-ray tomography (3D imaging) to study the mechanism and kinetics of dendrite formation and monitoring the growth of multiple dendrites in zinc-air systems [23]. Biton et al. (2017) studied the degradation of zinc-air batteries due to zinc dendrite growth *via* tomographic techniques and 3D imaging. They suggested that the

points of failure were located on the dendrite necks connecting to the base and that the dendrite's mechanical failure occurred at the bottom of the dendrites (Fig. 5(a)). Phase-field models have also shown that the bonding energy of zinc is stronger in a certain direction and hence, shaping the main tree branch of dendrite. During the cyclic processes, the smaller branches start to grow uniformly on the main stem of the dendrite (Fig. 5(b)). Different crystal planes correspond to different surface energies, implying different surface energy anisotropies. Moreover, dendrite growth is more facile at higher surface energy anisotropies (Fig. 5(c)). The dendrite study using *ex situ* XRD reveals that the crystalline orientation of the (002) plane of zinc is prevalent with the absence of the (101) plane, leading to the uniform nucleation of zinc. This also originates from the difference in the growth direction between the two planes when graphene oxide is loaded over the separator [26]. More recently, advanced approaches have been adopted in *in situ* and operando studies of dendrite formation (e.g. confocal laser scanning microscopy, transmission X-ray microscopy, transmission electron and nuclear magnetic resonance spectroscopy) (Fig. 5(d), 5(e)). The growth, regrowth, dissolution, and re-dissolution of dendrite formation as important parameters to allow for higher numbers of potential cycles have been recently studied via advanced operando visualization [27]. The initial dendrites generated at the high local current densities with rough surfaces (i.e. inhomogeneities) as well as progressing dendrites with various lengths on the shortest initiation time, were appeared on the electrode's surface. The growth behaviour depends on localized current and surrounding dendrites (i.e. primary, secondary, and ternary). Also, the dendrite thinning during discharge process leads to detachment from the electrode, in addition to the thinning of the zinc electrode. The regrowth of the dendrites during the charging process causes the new dendrites to attach to the prior dendrites. This leads to a complex and entangled network of dendrites. Denser dendrites are formed on the edges of the electrode due to the big deference in overpotentials between these edges and the zinc electrode's surface. In order to improve the cycling

9

performance of the rechargeable batteries, dendritic formation, as a critical factor, should be controlled. The reduction of dendrite growth is imperative for increasing battery's performance. Several dendrite formation prohibiting factors have been investigated. The studied factors have an important role in short-circuit and cyclic performance. This review discusses that the concentration gradient and the uniform distribution of the electric field can be tuned using various methods which can ultimately reduce dendrite formation and growth.
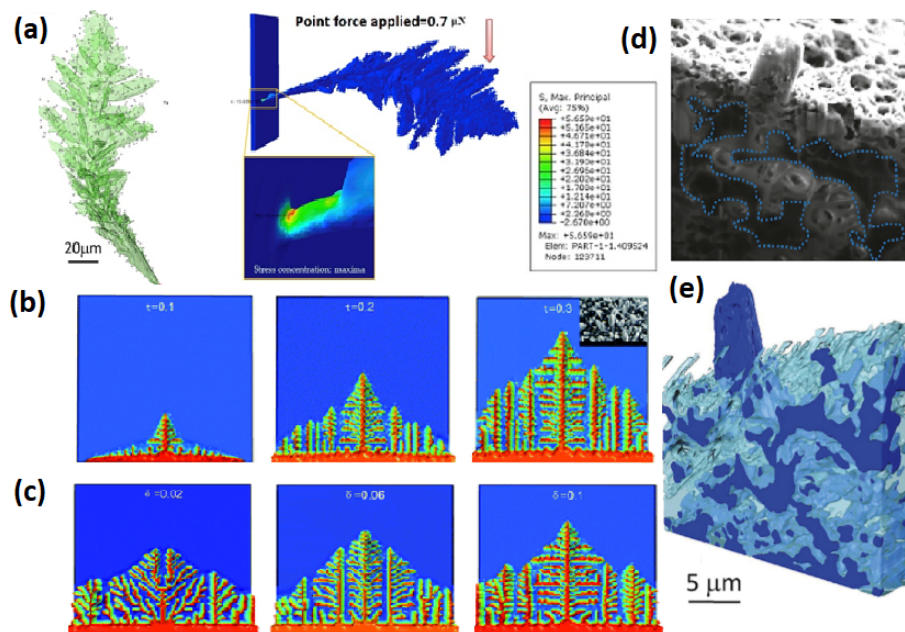


**Fig. 5.** (a) Two types of 3D images showing the growth of a single zinc dendrite, reproduced with permission from reference [24] Elsevier, (b) dendrite growth evolution of electrodeposited zinc (c) the effect of surface energy anisotropy on dendritic morphology [25], (d) cross-sectional of zinc deposits (separator) (e) (dark blue) zinc deposits and (light blue) zinc grown inside (porous separator) [27].

## 2.2 ZnO Formation & Hydrogen Evaluation Reactions

The concentration of electrolyte dictates the distribution of the discharge products; high concentration of alkaline solutions typically results in the dominant production of $Zn(OH)_4^{-2}$,

whereas the precipitation of Zn(OH)$_2$ crystals is linked to low concentrations of alkaline solutions [28]. The structural shape of the zinc electrode is affected by the build-up of internal stress. The high solubility of zinc in an alkaline media as zincate ions Zn(OH)$_4^{-2}$ negatively impacts the charging process. The high ion mobility facilitates the diffusion throughout the electrolyte, leading to non-homogenous deposition of zinc as well as the agglomeration of zinc on the edges. This may, in turn, deform the anode's structure. Novel zinc structures (*e.g.* porous zinc anodes, 3D zinc sponge, hyper-dendritic zinc foam and coatings layers) have been reported to be able to minimise this unwanted structural deformation [25-29]. Hydrogen evolution reaction (HER) occurs in aqueous electrolytes due to the low Zn/Zn$^{2+}$ potential ($-0.76$ V vs NHE) during each recharging cycle. The self-corrosion in zinc anodes generated *via* HER may result in gradual loss of capacity over time. In order to avoid the self-discharging event during the delivering process, a sticker is always coated over the air access holes to hinder air diffusion. The electrochemical window is determined by the energy gap between the lowest unoccupied molecular orbital (LUMO) and the highest occupied molecular orbital (HOMO). The electrochemical potentials of both electrodes should be between LUMO (conduction band) and HOMO (valence band). Zinc-electrolyte corrosion reaction takes place due to the electrochemical potential of Zn above the LUMO of the electrolyte [30]. The reaction between Zn and H$_2$O leads to the simultaneous production of Zn(OH)$_2$ and H$_2$ on the surface of the Zn anode (H$_2$ evolution reaction):

$$Zn + 2H_2O \rightarrow Zn(OH)_2 + H_2 \tag{2}$$

A large difference is observed between the actual energy density of zinc-air batteries (220$-$300 Wh/kg) and the corresponding theoretical value (1086 Wh/kg) due to low utilization rate of zinc [2,17,18]. This is a consequence of the passivation of the anode electrode (ZnO formation), following redox reactions of Zn in alkaline solutions:
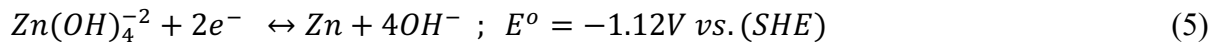
$$Zn + 4OH^- \rightarrow Zn(OH)_4^{-2} + 2e^- \tag{3}$$

$$Zn(OH)_4^{-2} \rightarrow ZnO + 2OH^- + H_2O \tag{4}$$
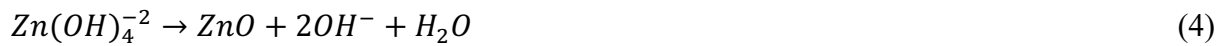
The discharge product, $Zn(OH)_4^{-2}$, generated at the saturation point during the discharge process, causes the decomposition of zincate ions to produce non-conducting ZnO. The white solid ZnO is then deposited on the surface of both electrodes and is not completely re-deposited during the charging process. Many approaches have been extensively proposed for reduction/suppression of the ZnO layer e.g. addition of surfactant to electrolytes, introducing chemical materials to dissolve/separate the dense layer and the adjustment of the electrolyte concentration. Zinc oxide (ZnO) precipitation acts as a passive layer and increases the internal resistance. This may terminate the discharge reaction and impact the anode utilization. Moreover, the reverse conversion of Zn metal is suppressed and the battery rechargeability is limited. Different mechanisms of passivation of the anode's surface have been reported in the literature. Sinu et al. suggested that the passivation layer comprised the inner layer (dense ZnO) and the outer layer ( $ZnO/Zn(OH)_2$) [31]. Liu et al. proposed another mechanism based on the amount of the contact time of zinc with the alkaline solution. These include the saturation time of zincate, the ZnO formation time, and the formation of dense ZnO layers [32]. A porous ZnO layers forms at low current densities without passivation surface. This is followed by facilitaed mass transfer of OH$^-$ ions across the ZnO layer. However, the formation of the dense ZnO layers create a passivate layer over the electrode at high current densities.

The equilibrium potential ($E_e$) between zinc and its various oxidized species depends on the pH of the solution (Pourbaix diagram). The zinc reactivity is also a function of the electrolyte pH (Fig. 6). Therefore, the described electrolyte limitations and the zinc-anode are closely interlinked. The two possible cathodic reactions *e.g.* hydrogen reduction and oxygen evolution reactions, can take place throughout the entire pH spectrum. Zinc is thermodynamically unstable in aqueous solutions and tends to dissolve ($Zn^{2+}$) along with

hydrogen evolution. Hydrogen evolution reaction consumes the charge (electron) during the charging process and reduces the columbic efficiency to <100% [33]. Zinc, zincate ions and zinc oxide are in equilibrium in electrolytes with pH=14 while ZnO particles precipitate when zincate exceeds its supersaturated concentration.

$$Zn(OH)_4^{-2} + 2e^- \leftrightarrow Zn + 4OH^- \; ; \; E^o = -1.12V \; vs. (SHE) \tag{5}$$
$$Zn(OH)_4^{-2} \leftrightarrow ZnO + H_2O + 2OH^- \; ; \tag{6}$$

Where, E° is the standard potential relative to the SHE at 25 °C.

However, stable Zn corrosion product *i.e.* Zn(OH)₂, is generated under neutral or slightly alkaline conditions. Zinc solubility rises with an increase in the pH. Zincate ions Zn(OH)₄ $^{-2}$ are formed while zinc oxide and hydroxides tend to dissolve at pH values > 9.
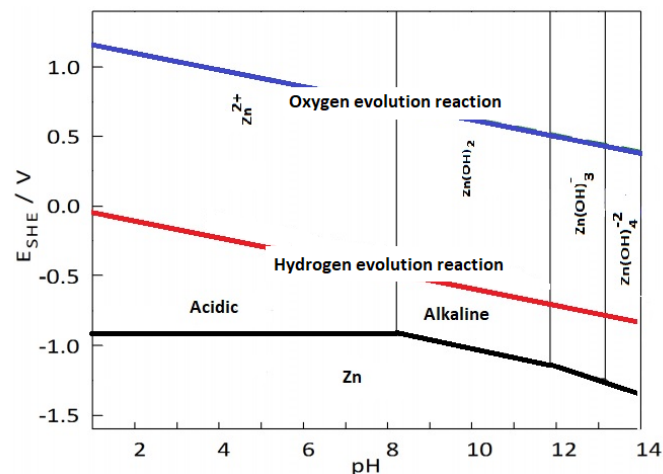


**Fig. 6.** Pourbaix diagram for zinc corresponding to different pH values in water [34]

In acidic electrolytes (*i.e.* pH 4–6), zinc can be dissolved to Zn$^{2+}$ (discharge) and is electrodeposited as zinc metal (charge). Surface oxides of zinc are not stable under acidic conditions. Corrosion and polarization characteristics of Zn in neutral-acid media (*i.e.* pH=3-5.8) have been associated with the formation of non-passivating porous oxide films.

$$Zn^{+2} + 2e^- \leftrightarrow Zn \; ; \; E^o = -0.76 \, V \; vs. (SHE) \tag{7}$$

The Pourbiax diagram shows that the redox potential of zinc is below the hydrogen evolution reaction (HER), and that the HER thermodynamically dominates at zinc redox potentials. Strategies to mitigate ZnO formation have been extensively studied to overcome the limiting achievable capacities and the cyclic lifetime issues. The studies reveal that regulating zincate concentration and controlling zinc dissolution are the key factors in reducing ZnO formation.

## 3. Liquid Electrolytes

The electrolyte serves as a medium for the migration of ions. It plays a key role in influencing the cell discharge potential, rechargeability and cell performance alike. A suitable electrolyte should have a high ionic conductivity ($>10^{-4}$ S/cm) and low electronic conductivity ($<10^{-10}$ S/cm), a high chemical stability, be low cost and assure safety. Typical alkaline electrolytes are extensively employed due to the desirable ionic conductivity of cation ions ($K^+$, $Li^+$, $Na^+$, $Mg^{2+}$). In addition, the high dielectric constant of water favours stable ionic species with the high solvating power. Less toxicity, higher ionic conductivity, non-flammability and inexpensiveness are typical advantages of aqueous electrolytes. However, the corrosion of the electrodes, the electrolyte evaporation (within a limited temperature range), the narrow electrochemical stability window, leakage and low thermodynamic stability of the metal-anode and finally, limitations for effective miniaturization are some of the key disadvantages [35,36].The operation of ZABs under ambient conditions (i.e. a $CO_2$ concentration of approximately 400 ppm) leads to the formation of carbonates. Precipitation of insoluble carbonates (*e.g.* $K_2CO_3$ or $KHCO_3$) originating from the reaction between KOH and the carbon content in air cathode and $CO_2$, can potentially block the air diffusion pathway of cathode, resulting in the deterioration of the battery's capacity. The crystallization of carbonates in the porous air electrode follows the reactions below [37]:

$$CO_2 + OH^- \rightarrow CO_2^{3-} + H_2O \qquad (8)$$
$$CO_2 + KOH \rightarrow K_2CO_3 + H_2O \qquad (9)$$
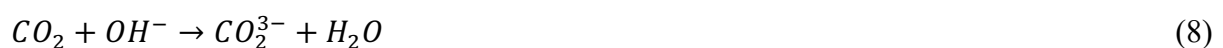
The effects of $CO_2$ contamination on ZAB's performance have been studied with various types of membranes. A fabricated electrospun membrane based on polystyrene (PS)/polyethylenimine (PEI) fibre has shown a $CO_2$ adsorption capacity of 3.42 mmol $CO_2$/g adsorbent and a better discharge capacity (i.e. 802 mAh/g) compared to that of the ZAB-free membrane (762 mAh/g) [38]. Moreover, the dissolved $O_2$ in LABs generated reactive intermediate species (e.g. superoxide radicals). The electrolyte decomposition leads to severe contamination of the lithium electrode which in turn, leads to the formation of a passivated film on the lithium electrode's surface. $CO_2$ contamination in metal-air batteries has been suggested as an alternative to metal-$CO_2$ batteries. $CO_2$'s solubility is 50 times that of the $O_2$ in organic solvents. Several reactions could take place between $CO_2$ and the active intermediate species $O_2^{\bullet-}$, and/or the discharge products (e.g. $K_2CO_3$). It has been proposed that $CO_2$, as the reactant, can be utilized in metal–$CO_2$ batteries. A primary Li–$CO_2$ battery with an electrolyte containing 1 M LiTFSI/1-butyl-3-methylimidazolium bis(trifluoromethanesulfonyl)imide, has successful demonstrated a discharge capacity of 2500 mAh/g with the following proposed reaction:

$$4Li + 3CO_2 \rightarrow 2Li_2CO_3 + C \tag{10}$$

The results in this research showed that the insulation coating of the discharge products could be improved by increasing the operation temperature to enhance the cell potential and the discharge capacity. The impact of a higher cathode's surface area with the use of appropriate electrolytes is more pronounced than an enhanced operation temperature [39]. Considerable research and development into neutral aqueous-, ionic liquids and non-aqueous (organic and solid-state) electrolyte-based batteries has been done in order to eliminate and/or minimize the problems associated with aqueous zinc electrodes [40,41]. Adding gel to aqueous liquid (Thixotropic gel electrolyte) has been suggested to improve the overall battery efficiency. The addition of gel to aqueous electrolytes increases the viscosity of the electrolyte resulting in the suspension of zinc powder. This can affect the porosity of zinc electrodes.

Othman et al. (2001) investigated the viability of the addition of hydroponics gel as additive to dilute alkaline solutions in a zinc-air primary battery [42]. They found that the hydroponics gel electrolyte was not effective in the electrochemistry of the zinc-air battery. Mohamad A.A (2006) indicated that a gel electrolyte by mixing KOH (6M) and hydroponics gel could be used as an electrolyte to eliminate leakage in zinc–air batteries [43]. Mitha et al. (2019) demonstrated significant improvement in the cycling performance and reliability of secondary aqueous $Zn/LiMn_2O_4$ batteries by employing a thixotropic gel electrolyte (PEG/fumed silica). Their analyses confirmed that the anode electrode was protected from excessive rate of zinc dendritic due to the optimum amount of PEG used in their work. This could affect the diffusion and reduction mechanisms of Zn ions . The use of high concentration alkaline electrolytes can enhance ZnO solubility and consequently, improve battery efficiency. This is linked to unstable passivation at high pH values. However, serious anodic corrosion limits the solution pH [44]. In liquid electrolytes, ion transport mechanisms are mainly based on the ionic mobility and the availability of electroactive species in liquid electrolytes. High ionic conductivities and low viscosities are imperative to facilitate accelerated ion transport. The basic assumption in the reported models for the ion transport processes are based on the physical diffusion of ions according to the Stokes–Einstein relationship. Molecular dynamic simulation suggests the exchange mechanisms based on the continual exchange of anions and solvents, or metal ions' hopping for the ionic conduction of highly-concentrated electrolytes with low ionic conductivities. It has been hypothesized that multiple coordinating sites (e.g. geometric/spatial) of solvents may hinder the formation of solvent-bridges with the ionic network structure of salts in highly-concentrated solutions - leading to the domination of the hopping/exchange-ion conduction [45].

Several approaches have been extensively reported for addressing the zinc dendrites/ZnO formation problem e.g. utilization of additives (electrolyte/electrode),

facilitating the mass transfer, covering/blocking the active sites involved in dendrite formation, improving electrode's surface area, and reducing the depositing current density. The use of additives and replacing non-aqueous or hybrid electrolytes with an aqueous electrolyte have been suggested as promising strategies to control Zn deposition. This can also foster the suppression of non-uniform Zn deposition. In the following sections, we will present a detailed overview of the alternative and recent approaches, reported to be able to effectively minimize the key issues associated with liquid electrolytes as outlined above.

## 3.1 Effective Electrolyte Additives

Use of additives is a promising approach to control zinc dendrite formation, zinc dissolution and also zinc electrodeposition. Low-cost electrolyte additives with high efficiencies are desirable for application in Zn-based batteries. Suitable additives facilitate the formation of a compact and uniform zinc electrodeposition, enhancing and improving the cyclability of batteries. Additives help to reduce material build-up on anode as a result of enhanced dissolution of the zinc deposition during each cycle. This, in turn, helps to maintain a constant concentration of zinc ions at a stable level. Also, additives facilitate the reduction of $Zn(OH)_4^{2-}$ solubility *via* the adsorption onto the active hydrogen evolution sites, leading to early ZnO precipitation [46]. Additives mainly fall into three categories of 1) organic additives (*e.g.* formaldehyde, perfluorocarboxylic acids, malonic acid, polyamine, tetraalkylammonium salt, surfactants , ethanol, DMSO and etc.), 2) metallic oxide additives (*e.g.* HgO, PbO, $Ga_2O_3$, $Tl_2O_3$, CdO, $Ca(OH)_2$ and $In(OH)_3$, $Bi_2O_3$, $In_2O_3$, $In(OH)_3$, CdO, $SiO_2$) and 3) structural electrode modifiers (*e.g.* Hg, Cd, Bi, Sn, In, Mg, Al, Ni, Pb) [47-49]. Schematic 2 shows a classification of various types of electrolytes in ZABs.

Schematic 2 Different types of used electrolytes in ZABs

It is believed that most additives are effective in improving batteries' performance. However, additives may also have several adverse impacts as well. These include increasing the impedance on the cathode electrodes, reaction with electrocatalysts, significant $H_2$ gas generation and precipitation of solid products over cathode's surface. Combinations of additives (i.e. cooperative effects) has been linked to a better cell performance than a single additive. The role of an additive depends on the type of the functional groups that are incorporated with individual additives. In order to enhance battery's performance, the property of the battery has to be tuned with the help of the associated functional group. The amount of additives should be carefully adjusted in order to prevent the occurrence of any undesired effects more especially, the cell impedance [50,51]. A good deal of effort is still required to be made in additive development for future optimum batteries' performance.

*3.1.1 Organic Additives*

Organic additives (commonly referred to as levellers, accelerator and/or suppressor) are employed in order to 1) modify the crystal growth, promoting the deposition on sites with low current density (*i.e.* cavities) and improving the adsorption on electroactive surface sites for

levelling deposition rates, 2) brighten the deposits, 3) shift the electrochemical mechanism from instantaneous to a more progressive one, 4) induce a reduction in grain size (low tendency to tree form) and 5) reduce stress and pitting. Organic additives are mostly used to inhibit dendrite formation. Organic acids, containing hydrophilic groups such as -COOH, can promote hydrogen bonding with water molecules along the Helmholtz layer formed on the electrode/electrolyte surface. The formed bonding *via* adsorbed organic molecules effectively blocks the electrode's surface and hinders the transportation of ions into the solution. This adversely inhibits growth within these regions [52]. The acidic additives such as phosphoric acid, tartaric acid, succinic acid and citric acid were tested in aqueous solutions of KOH (8.5M). The results indicated a noticeable rise in hydrogen evolution in the order of tartaric acid > succinic acid > phosphoric acid > citric acid. However, the prevention of dendrite formation followed the order of citric acid > succinic acid > tartaric acid > phosphoric acid. The prevention of dendrite formation is essential in order to effectively maintain the structure of anode after cycling processes. Additives not only reduce dendrite formation but they also increase the potential required for hydrogen evolution [53]. Nartey et al. 1994 investigated various organic corrosion inhibitors such as a-diphenylglyoxime, tripropylene glycol, diaminepyridine, polyethylene glycol (600) and polyethylene glycol (200) in rechargeable zinc batteries. The a-diphenylglyoxime and polyethylene glycol (600) corresponded to the best observed performance compared to the other additives used [54]. Thiourea and polyacrylamide were employed to modify the crystal orientation of nanocrystalline zinc in an aqueous zinc ammoniacal electrolyte during pulse electrodeposition [55]. Dimethyl sulfoxide (DMSO), a green solvent, exhibits a good stability throughout charge/discharge cycles with minimal hydrogen evaluation, while increasing the wettability of electrode surface [56]. The use of ethanol has been linked to an improvement of the discharge performance; the addition of 5–10% (v/v) ethanol could effectively suppress passivating layer formation on the active surface

of the zinc anodes [38]. Various types of tetra-alkyl ammonium hydroxides (TAAHs) have been reported to be effective additives in preventing zinc dendrite formation. TAAHs can significantly inhibit dendrite formation. The ability of inhibiting Zn dendrite formation is dependent on two key factors: the alkyl group size and the additive concentration. The mechanism of zinc dendrite formation can be attributed to the physical adsorption of TAAHs, covering the surface of the zinc electrode, and blocking active sites (more suitable for zinc dendrite). This happens as the alkyl groups can be attached to the zinc surface. Furthermore, increasing TAAHs concentration and the size of the alkyl groups may enhance the inhibition effect alike. The polarity of TAAHs (i.e. organic additives) also plays a key role. This effect is more pronounced with larger alkyl groups[57].

### 3.1.2 Polymer Additives

Polymer additives such PEG, PMMA, polycarbonate, polyaniline, polypyrrole and poly (vinyl acetate) restrict the dissolution of discharge products. These are effective in slowing down dendrite formation and deformation (*i.e.* structural change). Polymer additives polyethylene glycol (PEG 600) and polyoxyethylen alkyl phosphate ester acid (GAFAC RA600) have shown inhibition properties for zinc in strong alkaline solutions (8.5M). However, PEG600 has been reported to be more efficient than GAFAC RA600 [58]. Polyethylenimine (PEI) effectively hinders dendritic growth in rechargeable Zn batteries. PEI adsorption onto Zn surface slows down the Zn electrodeposition kinetics, and as a consequence, inhibits propagation of dendrite tips. Banik et al investigated the use of branched polyethylenimine (PEI) as additive to prevent dendrite growth (electrodeposition) in alkaline media [59]. They found out that a PEI concentration of 50 ppm was very effective as a result of the adsorption of additives onto the zinc anode surface which served as a physical barrier to zinc dendrite formation (Fig. 7). Degradation and polymerization of the polymers in alkaline

media may result in the neutralization of some functional groups such as carboxylic groups. This, in turn, may lead to the loss of hydrogen atoms from the negatively charged –COO–[60].
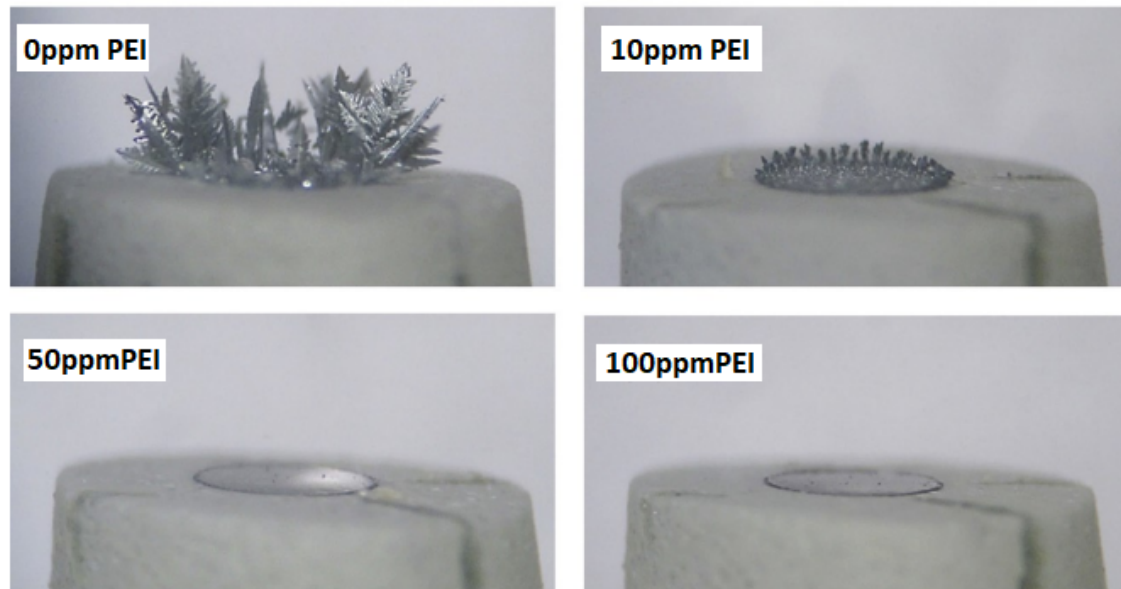


**Fig. 7.** the images of dendrite in Zn anode for various PEI concentration, Reproduced with permission from reference [59] Elsevier.

*3.1.3 Surfactant Additives*

Surfactant molecules are typically made up of a hydrophilic and a hydrophobic tail. The hydrophobic tail is a hydrocarbon, siloxane and fluorocarbon that can be oriented towards the electrode surface. Upon adsorption, it will create a barrier to prevent the surface accumulation of ions. Surfactants can therefore, help to avoid dendrite formation. They are widely employed to establish and maintain a smooth dendrites-free surface. Some surfactants have shown the ability to provide barriers on the electrode surface for the reactants (zincate) to balance their uneven deposition on the electrode surface [61]. The introduction of surfactants can significantly decrease the contact angle and increase the wettability between the electrode and the electrolyte. The effects of wettability are induced by changing the conductivity and viscosity of the electrolyte [62]. Adding 2% sodium dodecyl benzene sulfonate (SDBS) to

KOH solutions improved the discharge capacity of zinc anode by 35%. This was due to the formation of a loose and porous passive film, facilitating the diffusive ion exchange. The formed layer varied from dense (compact) to loose (porous) with the application of SDBS [63]. The effects of sodium dodecyl sulphate (SDS) and Triton X-100 surfactants was investigated in order to study dendrite formation in zinc-polyaniline batteries. A significant improvement was observed in the cycling performance (*i.e.* 80% retention after 38 cycles) with SDS and 79 cycles with Triton X-100, compared to additive-free electrolytes (*i.e.* 23 cycles) [64]. Using cetyltrimethylammonium bromide (CTAB), sodium dodecyl sulphate (SDS), thiourea (TU) and polyethylene-glycol (PEG-8000) organic additives showed distinctively different crystallographic orientation and surface texture. Except for CTAB, the use of SDS, TU and PEG-8000 improved the performance. In comparison, high capacity retention (*i.e.* 1000 cycle), low corrosion and low dendrite formation rates were recorded for sample containing SDS (Zinc-SDS). The majority of zinc-SDS surface planes were (103) and (002) and more inert in which the dendrite formation is much less likely [65]. Adsorption of dodecyltrimethylammonium bromide (DTAB) over zinc surface has proven to hold a positive impact of successfully inhibiting zinc corrosion with up to 80.2% recorded efficiency [66]. Non-ionic surfactants such as pluronic F-127 (P127) revealed an increase in the specific discharge capacity compared to anionic surfactant SDS. This was due to the presence of multiple anchoring groups per P127 molecule, creating superior interactions and enhanced adsorption with zinc anode, whilst SDS possess a single anchoring group with weaker surface adsorption [67]. These finding highlight the fact that the chemical structure of surfactants influences the formation of dendrite and the passivation layer. It has been reported that the use of non-ionic surfactants with multiple anchoring groups was advantageous as they bind onto the anode's surface, forming a passivation layer - unlike cationic and anionic surfactants. Moreover, anionic surfactants outperform cationic surfactants as the negatively-charged polar

group coordinates to zinc ions at the electrode/electrolyte surface to reduce ZnO formation. However, the positively-charged polar group of cationic surfactants exhibits weak interactions with zinc ions, leading to an increased formation of ZnO[67-69].
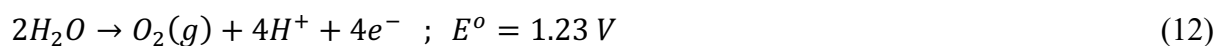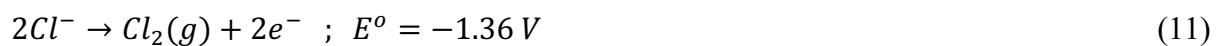
*3.1.4 Electrode Additives*

In addition to electrolytes, additives can be also added to anodes in order to improve the cyclability performance. Carbon materials, bimetals and polymers have been studied as additives for Zn electrodes in order to decrease dendrite formation. Modification of zinc electrodes is a promising approach to negate the adverse effects of dendrite growth and structural change. Fabrication of anode comprising zinc and polymer has been suggested to inhibit the growth of dendrites. Porous zinc electrode coated with polyaniline was found to be useful in stabilizing the capacity of the electrode (*i.e.* cycling). The fibrous network of the coated polymer allows the flow of the OH⁻ ions and while restricting zincate ion diffusion [70]. Electrochemical polymerization of pyrrole on zinc foil in aqueous medium (sodium tartrate) has led to the production of less-corrosive zinc in alkaline media [71]. The addition of bismuth (Bi) (10% wt) and calcium (Ca) into a pasted zinc electrode enhanced the discharge behaviour. Bismuth improves electronic conductivity while little structural change and small dendrite growth were observed in calcium zincate as a result of low solubility [72]. Alloy of indium, nickel and zinc with an optimum composition of 2.5%, 7.5% and 90%, respectively, resulted in minimal dendrite formation with a reversibility of more than 100 cycles [73]. Jo et al. (2014) studied the effect of 1 and 3 wt% Bi and Ni as additives on a gel-type zinc electrode. The Bi-containing zinc anode showed a better discharge performance compared to the Ni-containing counterpart. Unlike Bi, the use of Ni in pellet-type electrode was a success in corrosion inhabitation, whereas Bi proved to be effective in gel-type electrodes in Zn-air batteries [74]. Among the intrinsically conducting polymers, polypyrrole (PPy) and polyaniline (PANI) were found to be most suitable due to their wide range of conductivities, tuneable properties and

high stabilities. Conductive polymers as additives can be added to anode to improve the overall performance of rechargeable batteries. PANI-coated zinc was used to mitigate the self-discharge behaviour, inhibit HER and corrosion reactions by preventing direct contact between zinc and the KOH electrolyte [75]. Electrodeposited ZnO on carbon mesh with a protecting layer (*i.e.* Ionomeric Hydroxide-Conducting Polymer) has yielded excellent cycling stability. It is a consequence of the diffusion of zincate species into the electrolyte. The composite electrode showed a high utilization rate of the active material (~93%), leading to an enhanced capacity retention [76]. Nanoporous $CaCO_3$ coated zinc provides a uniformly of zinc dissolution and deposition due to the high porosity of $CaCO_3$ layer. The uniform and high porous $CaCO_3$ layer induces steady flux of electrolyte and zinc dissolution/precipitation rate over the zinc surface [ Kang 2017]. Coating of zinc surface or inducing additives into zinc electrode enhances zinc electrode's performance. This may improve electrical conductivity, surface structure and current distribution - which may prevent dendrite growth. The migration of zincate ions can be limited in order to minimize the deformation of the electrode and irreversible reactions (i.e. ZnO).

## 4. Neutral Electrolytes

The adsorption of atmospheric $CO_2$ in electrolyte initiates the formation of carbonates ($CO_3^{2-}$). This can poison electrolytes and ultimately, reduce the lifetime of zinc-air batteries. Integration of $CO_2$ filters and regulating electrolyte's pH at about neutral values could slow down the undesirable carbonation process. $ZnCl_2$–$NH_4Cl$, one of the most commonly used neutral electrolyte, has been used in zinc-based LeClanché batteries for more than 100 years. The neutral electrolytes often have lower ionic conductivities and low $OH^-$ concentrations. As a result, both oxygen evolution (OER/charge) and oxygen reduction (ORR/discharge) reactions are kinetically slow. Bifunctional air catalysts have been broadly used in order to improve ORR/OER reactions in both alkaline media and neutral electrolytes. The electrolyte pH and its

composition affect the observed reaction mechanism and performance of the bifunctional catalysts. Clark et al. (2017) predicted that the neutral electrolyte ZnCl₂/NH₄Cl became acidic on the bifunctional catalyst surface (*i.e.* charging process) due to the slow diffusion of buffering species (*i.e.* NH₃), eventually impacting the catalyst's lifetime [77]. Electrolytes containing NH4C1, KC1, SnCl₂ SnCl₄, BiCl₃, HgCl₂, Hg₂Cl₂, PbCl₂, PbCl₄, CdCl₂, ZnCl₂, MgCl₂ NH₄Cl, LiCl, ZnCl2, NH4NO3, (NH₄)₂SO₄, NH₄OH KNO₃, K₂SO₄, Na₂SO₄ and Na₂SO₃ are considered neutral and can be used to mitigate corrosion and offer high buffering capacities and wide working potential windows (*i.e.* <2V) [2,3,78-80]. They can reduce dendrite formation as well as mitigating electrolyte carbonation. The pH of the electrolyte can be adjusted to 7 with KNO₃, KCl, Na₂SO₃, K₂SO₄ and Na₂SO₄ while it can be regulated to <5 using ammonium salts (*e.g.* NH₄Cl, NH₄NO₃). Chloride-based electrolytes are found unsuitable for rechargeable metal-air batteries due to corrosion once anodic potentials are applied. Chlorine evolution reaction (charging presses) is an undesirable side reaction, leading to the formation of acids such as HCl and HClO, adversely impacting oxygen evolution reaction [81]:

$$2Cl^- \rightarrow Cl_2(g) + 2e^- \quad ; \quad E^o = -1.36\,V \tag{11}$$
$$2H_2O \rightarrow O_2(g) + 4H^+ + 4e^- \quad ; \quad E^o = 1.23\,V \tag{12}$$

In order to reduce chlorine evolution, some inorganic additives such as IrO₂, CoCl₂, TiO₂-supported RuO₂ and urea have also been suggested to prevent chlorine and/or hypochloride evolution [82]. Depending on the cation type, chloride salts can influence products (charge/discharge), chlorine evolution and hydrogen evolution reactions. It has been reported that the concentration of the neutral electrolytes affected the discharge products; amorphous zinc chloride hydroxide monohydrate (ZnCl₂·4Zn(OH)₂·H₂O) at low NH₄Cl concentrations has been detected, whereas at high NH₄Cl concentrations, the formation of crystalline zinc diammine chloride (ZnCl₂·2NH₃) has been observed. Moreover, the

crystalline phase poses a higher risk of passivation compared to the amorphous phase [83]. Zinc ions ($Zn^{+2}$) can be complexed with other ions such as $NH_3$ and $Cl^-$ (Fig. 8), depending on the electrolyte pH and the ionic concentration [77]. These researchers demonstrated a novel framework for modelling the performance of Zn-air batteries based on a neutral electrolyte ($ZnCl_2$ -$NH_4Cl$), by taking into account the pH stability, in order to pinpoint the optimum composition of electrolyte as well as informing the cell design.
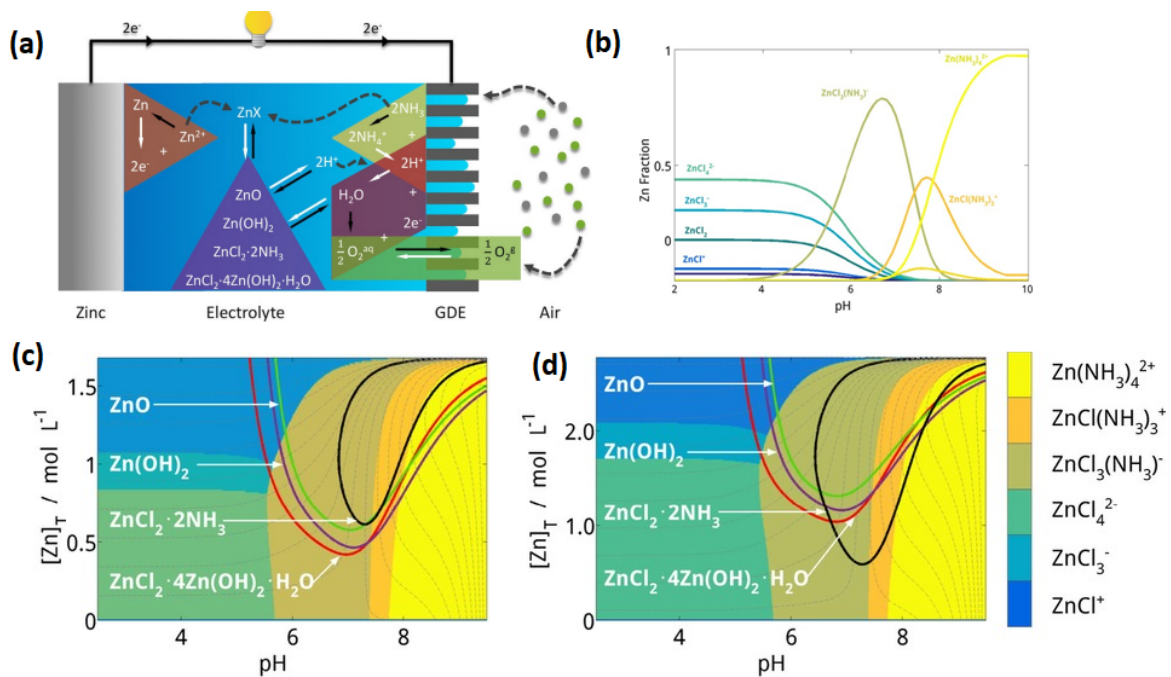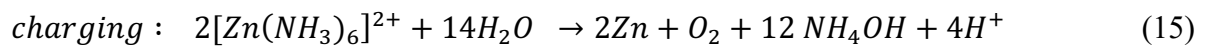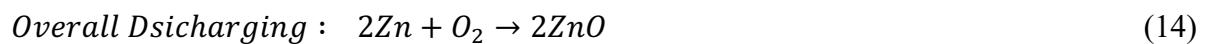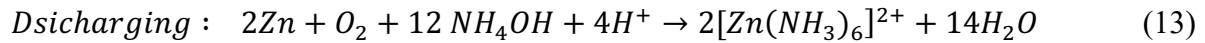


**Fig. 8.** (a) Operational diagram of $ZnCl_2$–$NH_4Cl$ electrolyte in a zinc–air battery with ZnCl2–NH4Cl electrolyte, (b)speciation of the $Zn^{2+}$ ion versus pH on a neutral electrolyte ($ZnCl_2$-$NH_4Cl$), Discharge product solubilities and zinc complexes (c) 3.36 mol/L chloride concentration and (d) 5.54 mol/ L chloride concentration [77]

By employing neutral-pH electrolytes (and consequently, reducing zinc solubility and $CO_2$ absorption), the cycle life of the secondary zinc-air batteries can be improved, owing to the mitigation of dendrite formation and the reduction of carbonates' precipitation. However, the power performance is limited due to their low ionic conductivities at room temperature and corrosion, especially in coin-type cells [2,3,84]. Goh et al. (2014) studied neutral electrolytes

$ZnCl_2$-$NH_4Cl$ with polyethylene glycol and thiourea additives in a rechargeable zinc-air battery. The addition of PEG and thiourea inhibited zinc deposition from the chloride baths. They found these additives more beneficial in the mitigation of zinc dendrite formation. The reactions in the near-neutral chloride electrolytes can be described as follows [85]:

$$Dsicharging: \quad 2Zn + O_2 + 12\,NH_4OH + 4H^+ \rightarrow 2[Zn(NH_3)_6]^{2+} + 14H_2O \qquad (13)$$

$$Overall\ Dsicharging: \quad 2Zn + O_2 \rightarrow 2ZnO \qquad (14)$$

$$charging: \quad 2[Zn(NH_3)_6]^{2+} + 14H_2O \rightarrow 2Zn + O_2 + 12\,NH_4OH + 4H^+ \qquad (15)$$

$$Overall\ charging: \quad 2ZnO \rightarrow O_2 + 2Zn \qquad (16)$$

Amendola et al. (2016) investigated rechargeable Zn-air batteries using a neutral electrolyte with charge and discharge voltages of 2.1 and 0.9 V, respectively [81]. The integration of MnOx catalyst on carbon paper and neutral chloride-based electrolytes enhanced the cycling stability (*i.e.* 90 days) due to minimal carbonation and reduced carbon corrosion (air cathode) in rechargeable Zn-air batteries [80]. Molten-salt electrolytes offer high energy- as well as power densities, resulting in the avoidance of some issues associated with hydrogen evolution and Zn dendrite formation. The use of molten $Li_{0.87}Na_{0.63}K_{0.50}CO_3$ eutectic electrolyte corresponded to a high coulombic efficiency over 110 cycles in a rechargeable zinc-air battery [86]. A schematic representation of the zinc molten air battery's charge and discharge processes is presented in Fig. 9. The neutral electrolytes can potentially overcome some of the problems including carbonation formation and corrosion issues. Nevertheless, identifying the optimum composition to increase ionic conductivity still presents itself as a major challenge.
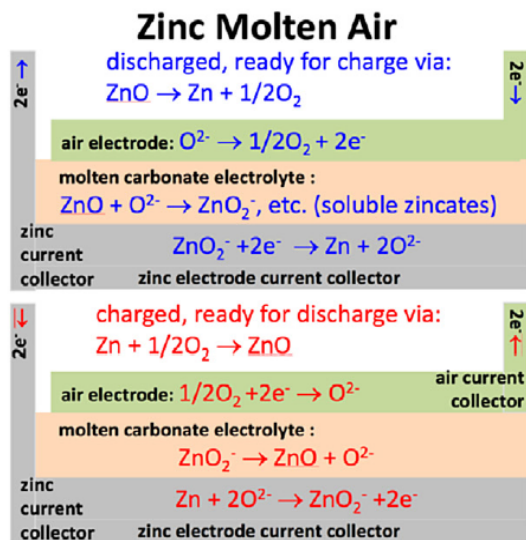
**Fig. 9.** the schematic representation of the zinc molten air battery, Reproduced with permission from reference [86] Elsevier.

## 5. Non-aqueous electrolytes

### 5.1 Solid electrolytes

There have been some efforts to replace non-aqueous electrolytes e.g. polymer-based or solid electrolytes. As a result, research has been undertaken to address the challenges facing the application of solid state, solid polymer- and/or gel polymer-electrolytes in metal-air batteries. The use of polymer matrix in composite solid electrolytes improve the flexibility of solid composite electrolytes. It can reduce resistance at the electrode-electrolyte interface. It also simplifies the large-scale manufacturing processes. Solid-state electrolytes can be inorganic solid oxide-, solid sulphide - or solid nitride-based. They can also be developed based on organic solids and a possible classification of solid electrolytes shown (schematic 3). The solid electrolytes serve two key roles; it acts as an aqueous electrolyte (for ion conduction) and as a separator (*i.e.* preventing internal short-circuit). Different approaches have reported to fabricate polymeric electrolytes by impregnating basic polymer backbone with $OH^-$ functional group and by integrating alkaline salts into the inert polymer matrix [87-89].

28
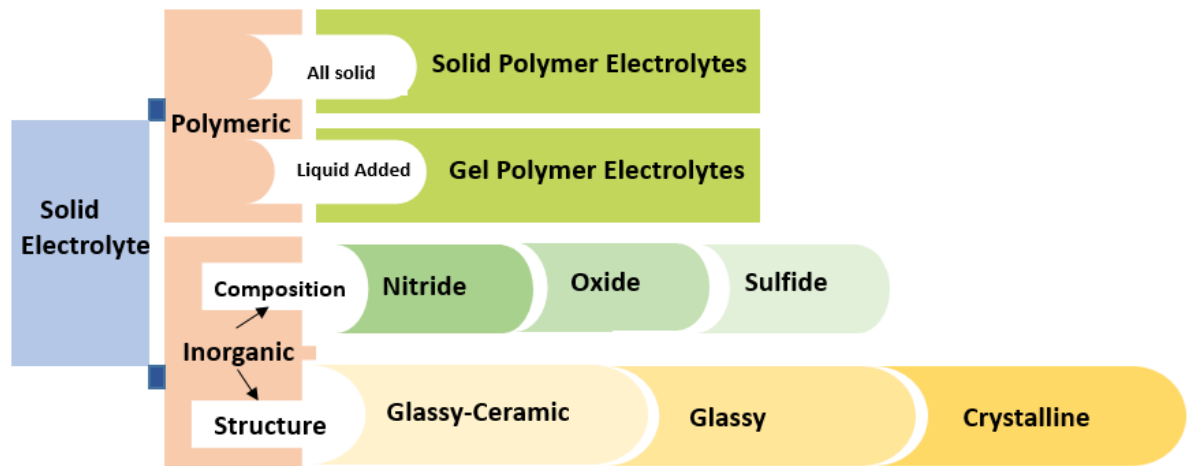
Schematic 3 A possible classification of solid electrolytes

*5.1.1 Inorganic Solid Electrolytes*

Ceramic-based solid electrolytes haves demonstrated several advantages including high energy densities, negligible electrolytes leakage, flame resistance, good reliability, high electrochemical stability, long cycle performance and feasibility for large-scale batteries. The oxide-based electrolytes show good stabilities under ambient conditions with large interfacial resistance between the solid electrolyte and the electrode. The ionic conductivity of solid oxide electrolytes is $<1\times10^{-4}$ S/cm at room temperature which is not suitable for applications in batteries. Also, a dense and uniform electrolyte is challenging to directly produce at high temperatures [90,91]. Unlike oxide-based electrolytes, solid sulphide-based electrolytes have low thermodynamic stabilities (in ambient conditions and even in polar solvents). The presence of sulphides can lead to the generation of toxic $H_2S$ when exposed to moisture. Nevertheless, these electrolytes have shown excellent ionic conductivities of around $1\times10^{-2}$ S/cm at room temperatures. Sulphide groups can corrode the grain boundaries, causing the appearance of cracks in ceramics as well as solid-state electrolytes [92]. Nitride-based electrolytes demonstrate ionic conductivities $<10^{-3}$ S/cm at room temperatures but low electrochemical decomposition potentials and poor stabilities hinder their employment in practical applications

[93,94]. The conductivities of the solid-state electrolytes are induced *via* the ionic motions across crystalline lattice sites. Unlike liquid electrolytes, solid electrolytes fail to infiltrate into cathode pores and therefore, the accumulation of electrostatic charges on electrodes/electrolyte interface causes considerable polarization of electrodes. By the addition of polymer to solid-state electrolytes, stability, performance and electrode/electrolyte interface features can be improved [95]. Due to insufficient ionic conductivity at room temperatures, fragility, instability and poor interfacial contacts, their rapid growth is still ongoing business.

The interfacial resistance, a critical parameter, dictates the corresponding commercial applications. The interface resistance is directly related to the chemical stability of the materials at the electrolyte/electrode interface. Recent studies have reported on reducing the interfacial resistance via several proposed methods e.g. coating/sputtering transition layers (polymers as soft contact, silicon, $Al_2O_3$, graphene oxide, $Li_3N$), employment of advanced structural design of the anode metal (i.e. 3D) to made uniform deposition/discharge cycles, use of suitable electrolytes for enhancing wetting ability over anode electrode, modifying internal particles in the cathode to improve the ionic conductivity inside the cathode, and fine-tuning the thickness of the cathode's layer [96].

### 5.1.2 *Organic Solid Electrolytes*

Organic solid electrolytes have several advantages over their inorganic counterparts. These include better flexibility, great interfacial contacts between the electrolyte and the electrode, lightness and simplified large-scale fabrication. Electrolytes with a combination of polymers and salts are known as salt-in-polymer (or polymer-in-salt) electrolytes depending on compositional ratios. Solid polymer electrolytes (SPE) have been linked to better operating temperature ranges, electrical recharge-abilities, good mechanical strengths, simple fabrication, negligible leakage and being solvent-free. However, several disadvantages such as low ionic conductivity (*i.e.* $10^{-8}$ to $10^{-5}$ $Scm^{-1}$), the instability of the electrode/electrolyte

interface and salt depletion at the electrode/electrolyte interface are yet to be addressed to pave the way for practical applications in metal-air batteries [3,90]. SPE contains a salt with a low lattice energy and hosts a polymer with a high dielectric constant to facilitate ionic dissociation and transportation [96]. The salts act as a source of mobile ions, while the polar groups of the polymers are bonded with ions (cations, anions), according to the Lewis acid–base theory. A solid electrolyte with the high flexibility of polymer chain and fast segmental dynamics can be formed by adding conductive salts to the polymer matrix. The function of the amorphous phase depends on the salt content as well as the preparation method. The selection of polymer host depends on the existence of polar functions with good proton donors and a low hindrance to bond rotation [90, 97]. The nature of the functional groups attached to the polymer backbone (*e.g.* OH, CO, $NH_2$, $CH_3$, F, Cl), molecular weight, compositions and distance between the functional groups, nature and charge of metal cation, degree of branching and counter ions are the important factors influencing the polymer-metal ion interactions [98].

The optimum salt concentration is key to achieve high performance. This is due to the fact that a strong interaction between ions (salt) and polymer results in further dissolvement of the salt. However, high salt concentration obstructs ionic movements. Therefore, both weak ions' coordination to the polymer chains and segmental motions, contribute to fast ionic transport. For this reason, excessively high concentrations of ions may lead ionic aggregation, hampering the ionic movements. There have been also technical challenges in establishing an accessible metal-ion path at solid electrolyte interface (SEI) in batteries. It has been reported that the SEI layer on the anode surface is continuously regenerated by the spontaneous reactions between reactive anode (metal) and organic electrolytes and breaks during cycling. The SEI layer shows some advantages as it is permeable to metal ions and prevents further corrosion. However, dendrite formation takes place as a result of anode deposition and dissolution [99,100]. The SEI is a passivating layer formed on the anode surface, primarily

during the first cycle, and originates from the mismatch between the electrochemical stability window (*i.e.* oxidation/reduction limits) of the electrolyte and the electrochemical potential of the electrodes. The SEI usually comprises the products that are generated from solvent reduction in the electrolyte and salt degradation. A stable passivating SEI layer protects the electrode from further reactions with the electrolyte, thereby, avoiding undesired electrolyte consumption. However, it also limits the kinetics of the ion transport processes. Therefore, understanding the formation mechanism as well as the chemical composition of the SEI is the key to improve the performance of batteries. The reversibility of batteries is limited due to the poor buffering properties of the SPEs for the zincate ion discharge products. This zincate builds up during the discharge and leads to passivation, imposing limitations on the SPEs during subsequent charging. This makes it difficult to maintain an ideal surface contact between the metal anode and the solid electrolyte membrane [101,102].

Due to the low ionic conductivity in SPEs at room temperatures, several strategies have been proposed to achieve a lower glass transition temperature ($T_g$) and thus, enhance the ionic conductivity. The polymer should have the ability to easily dissolve salts. Consequently, the polymer should have high electron-donor characteristics and high dielectric constants. The ideal polymers should have high concentrations of polar groups (ether (-O-), sulphide (-S-), amine (-N-), phosphine (-P-), carbonyl (C=O) and cyano (C=N)). They should have a flexible backbone and present low steric hindrance for bond rotations and have appropriate distance between coordinating centres. They must be feasible and economical to synthesise and process. The mechanical properties and process ability of polymer materials, as hosts to the SPE, can be determined using the glass transition temperature. Both crystalline and amorphous phases are detected in a polymer electrolyte; however, the amorphous phase has a bigger contribution in ionic transport. This is due to the fact that the polymeric chain motion is not active in the crystalline phase, while the amorphous phase, holds free activated chain segments (at T>Tg)

as shown in Fig 10. Crystallization can effectively reduce the fraction of the amorphous phase, producing more tortuous pathways for ion transport and restricting chain mobility. Therefore, in order to reduce/optimise the crystallinity of polymers and improve the ionic conductivity, various methods have been suggested. These include the addition of plasticizers, blending of polymers, grafting and crosslinking modification [103-105]. Dispersion of various types of fillers such as inorganics, ceramics, inert and organic–inorganic hybrids are widely proposed as an effective approach to increase the segmental motion ability in polymers and improve the basic physical properties of pure polymers. Similarly, branch-structured (or star-like polymers) are intrinsically amorphous and therefore, their addition can be an effective way to enhance the movement of polymeric segments and ultimately, increase the ionic conductivity [2,3,90].
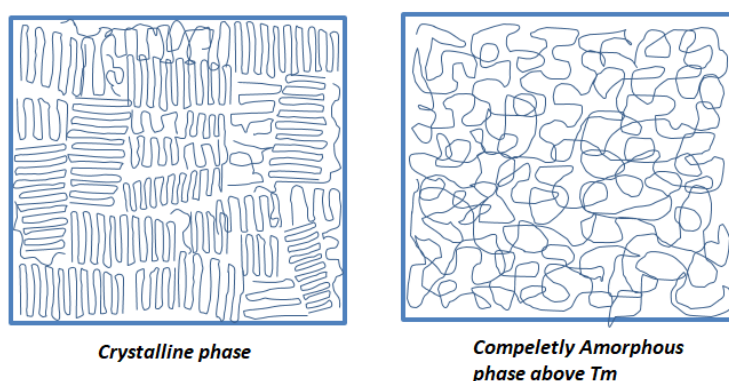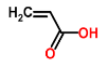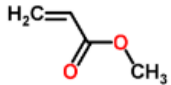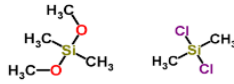


**Crystalline phase**          **Compeletly Amorphous phase above Tm**
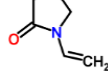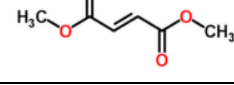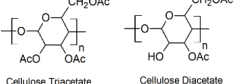
**Fig. 10.** Crystalline and amorphous regions of polymers

In comparison, poly(ethylene oxide) (PEO) and polyvinyl alcohol (PVA) polymers are widely used to fabricate polymer-based electrolytes. However, their low ionic conductivities render them unsuitable in batteries [106]. PEO, as the polymer host, usually form stable dry complexes and the oxyethylene group ($-CH_2-CH_2-O-$) and the polar groups ($-O-$, $-H-$, $-C-H-$) in the polymer chains can readily dissolve in solvents and ionic salts alike [107]. In order to minimise the crystallization of PEO for better ionic conductivity, several techniques have been reported. These include the blending of PEO with inorganic substances, copolymerization and cross-linking. Table 1 summarises a list of different types of polymers generally used as host polymers in SPEs. The ion conduction mechanism in SPE depends on the polymeric structure.

Long-range movement of polymer chains due to entanglement can also restricts ionic conduction. The conduction of ions through a unique segmental motion can initiate and facilitate ion-hopping process. The metal ions can be coordinated by oxygen on the PEO backbone. The movement of the metal cations is initiated by breaking bonds and subsequently, forming new bonds with the neighbouring coordination sites - assisted by the local reorganization of the PEO segments [108].

**Table 1** Various types of polymers (*i.e.* host polymers) used in SPE fabrication

| Polymer | Chemical structure | SMILES | Solubility Parameter $\delta$ MPa$^{1/2}$ | Tg $^{\circ}$C |
|---------|-------------------|--------|-------------------------------------------|---------------|
| Poly(ethylene adipate)/PEA |  | OC(=O)CCCCC(=O)O.OCCO | 20.4 | 43 |
| Polylactic acid/PLA |  | OC(=O)C(O)C | 20.3 | 59 |
| Poly(acrylonitrile)/PAN |  | C=CC#N | 26.3 | 110 |
| Poly(methacrylonitrile) /PMeAN |  | CC(=C)C#N | 23.3 | 115 |
| Polymethacrylamide/PMI |  | CC(=C)C(=O)N | 23.2 | 213 |
| Poly(acrylamide)/PAM |  | OC(=N)C=C | 25.9 | 165 |
| Poly(N-isopropyl acrylamide) /PNIPA |  | C=CC(=O)NC(C)C | 23.5 | 130 |
| Poly(vinylalcohol)/PVA |  | C{-}(OC(=O)C)C{n+} | 30.5 | 80 |
| Poly(vinyl acetate*)*/PVAc |  | CC(=O)OC=C | 19.6 | 34 |
| Poly(dodecyl methacrylate) |  | CCCCCCCCCCCCOC(=O)C(=C)C | 16.8 | -55 |

| /PDMA | | | | |
|---|---|---|---|---|
| Poly(acrylic acid)/PAA | | OC(=O)C=C | 21.3 | 101 |
| Poly(methyl acrylate)/PMA | | COC(=O)C=C | 19.6 | 7 |
| Poly(dimethylsiloxane) /PDMS | | C[Si](C)(Cl)Cl, CO[Si](C)(C)OC | 15.3 | -124 |
| Poly(butyl vinyl thioether) | | CCCCSC=C | 17.5 | -20 |
| Poly(vinylpyrrolidone)/PVP | | C=CN1CCCC1=O | 23.9 | 173 |
| Poly(dimethyl fumarate)/ PDMF | | COC(=O)/C=C/C(=O)OC | 19.9 | 100 |
| Cellulose Acetate/CA | | | 24 | 187 |

### 5.1.3 Improving Ionic Conductivity

The low effective carrier mobilities in the crystalline region of polymers below the melting temperature can be enhanced by stabilizing the highly conductive amorphous matrix with fillers. Polymer electrolytes containing fillers such as inert fillers (TiO$_2$, SnO$_2$, MgO, Al$_2$O$_3$, ZrO$_2$ and SiO$_2$) that are not directly involved in the ion conduction process, as well as active fillers (Li$_3$N) that play a role in ion transport, have been developed to enhance the segmental motion of the host polymer in order to increase ion conduction and improve the mechanical strength of electrolytes [109-111]. Appropriate dispersion of particles in the polymeric matrix results in an alternation of the polymer–particle interface and brings about more homogeneity. The improvement of conductivity as a result of the addition of fillers can be explained by two mechanisms: (i) fillers act as cross-linking centres to decrease the polymer

crystallinity in order to facilitate the segmental motion and (ii) the strong Lewis acid−base interaction between the surface chemical groups of fillers and electrolyte ion species causes an increase in salt dissociation and stabilizes the anions [112,113].

Comprising several phases, titanium Oxide ($TiO_2$) fillers are sub- to several microns in size. The addition of titanium oxide containing $Ti_2O_3$, $TiO$ and $Ti_2O$ into the (PEO) polymer electrolyte improves the ionic conductivity due to the change of -C-O-C- vibration and ionic structure of polymer electrolytes by the decrease in crystallinity of PEO polymer electrolytes. The redox couple mobility between poly (ethylene oxide) chains increases due to the addition of the $TiO_2$ fillers. A high ionic conductivity of $1.8 \times 10^{-4}$ S/cm was reported after the addition of 7.5wt% titanium dioxide ($TiO_2$) as filler to PAN [114]. A combination of $TiO_2$ with various types of polymers for the improvement of ionic conductivity is presented in Table 2. It shows that the addition of $TiO_2$ results in a change in the ionic conductivity between $10^{-3}$ and $10^{-5}$ S/cm. Silica particles ($SiO_2$) have been mostly suggested as effective fillers to mitigate the formation of passivation layers, enhancing the mechanical properties and ionic conductivities of polymer electrolytes. It was observed that the surface chemistry of fillers played an important role in the ionic conductivity [115,116]. The conductivity of solid polymer PEO-based electrolytes has been raised to $2.3 \times 10^{-5}$ S/cm by adding a nano-sized inorganic filler ($SiO_2$). The inorganic filler may change SPE by hindering the crystallization of PEO and the simultaneous re-arrangement of dipoles in a direction parallel to the applied electric field in the composite electrolytes [117]. An alternative approach to $SiO_2$ modification using acid/base properties has demonstrated excellent dispersion of nanoparticles *via* the interaction between the acidic hydroxyl groups in silica nanoparticles with the polymer functional groups. Sulfonated silica nanoparticles prepared with sulfonated silane, were used to synthesise particles containing specific ionic groups. The ionic conductivity enhancement using different fillers is a function of the type of salt. The maximum increase of ionic conductivity has been

recorded to be achieved with $10^{-15}$ wt% concentration of the nanofillers in SPEs at room temperatures [118]. High ionic conductivities ($>10^{-4}$ S/cm) can be obtained for a filler composition of $>30$ wt%. This, however, may result in poor processability, mechanical properties and cell performance [119]. The use of polyurethane acrylate (PUA)-based polymer electrolyte, containing nano-$SiO_2$, significantly improved the interfacial stability (cathode/electrolyte) and cyclability (300 cycles) with a columbic efficiency of 100% [120].

$Al_2O_3$ as a ceramic filler can also improve conductivity by promoting the structural changes in the polymer network. Studies have suggested that $Al_2O_3$ is capable of providing additional sites for the migration of ionic species through transient bonding with O/OH groups on the filler's surface. Adding 5 wt.% aluminium oxide ($Al_2O_3$) to PEO increased the ionic conductivity to about $3.3 \times 10^{-4}$ S/cm [121]. Croce et al. (2001) studied the effects of the use of $Al_2O_3$ nanoparticles with different surface characteristics (*e.g.* acidic, neutral and basic) on the modification of PEO [122]. The acidic/neutral $Al_2O_3$-based SPEs showed better conductivities compared to basic $Al_2O_3$-based SPEs. The perceived mechanism based on the specific Lewis-acid interactions is described in Fig. 11.
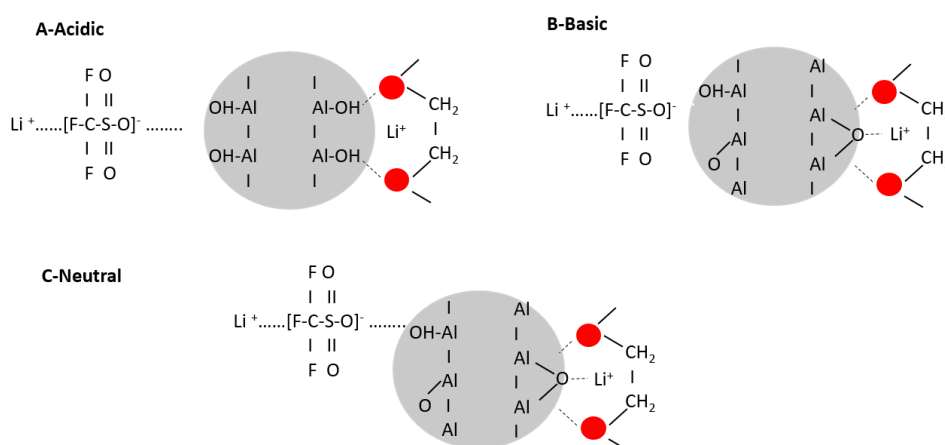


**Fig. 11**. A schematic of three types of surface interactions with $Al_2O_3$ nanoparticles, Reproduced with permission from reference [122] Elsevier.

Similar behaviour can be assumed for acidic and neutral $Al_2O_3$ due to the formation of hydrogen bonds with oxygen and anions to promote the dissociation of salts and the weakening of the cation-polymer coordination. Unlike this mechanism, basic $Al_2O_3$ can interact with cations. Jayathilaka et al 2002 claimed that there was no direct reaction between polymeric chains and fillers in which $Al_2O_3$ particles were able to interact with both anions and cations to facilitate ion hopping with an enhancement in ionic conductivity in order of: acidic > basic > neutral > weakly acidic > filler free [123]. Egashira et al. (2006) investigated $Al_2O_3$ filler-based solid polymer electrolytes treated with acid and alkali solutions. The surface-treatment of $Al_2O_3$ influences the ionic conductivity of SPE and the current density of the electrode [124]. Dissanayake et al. (2003) studied the effect of concentration and grain size of alumina fillers on the ionic conductivity enhancement of PEO. The optimum nano-porous alumina grains (5.8 nm pore size, 150 $m^2$/g specific area, 15 wt.% filler concentration) could best improve the ionic conductivity *via* Lewis acid–base type surface interactions of ionic species with O/OH groups on the filler surface [125]. PVA-PEG-NaI-$Al_2O_3$ electrolytes have been associated with the maximum dielectric constant compared to PVA-PEG-AgI-$Al_2O_3$ and PVA-PEG-MgI-$Al_2O_3$. This is linked to the enhancement of ionic conductivity [126].

Graphene oxides have large surface areas, high ionic conductivities, insulating properties, low interfacial resistances, good thermal stabilities and mechanical strengths. These features make these materials promising in the improvement of electrolytes' performance. Two-dimensional graphene oxide sheets have been suggested as filler to improve both ionic conductivity and tensile strength. Graphene oxide sheets contain oxygenated functional groups *e.g.* epoxy, hydroxyl and carboxyl which can facilitate ionic transport. Graphene oxide sheets can interlink to create a network with the polymer composite electrolyte. This will, in turn, sustain continuous ion conduction. The reducing crystallinity of polymer matrix and increasing free-volume leads to an increase in liquid uptake and polymer segmental mobility due to add

GO in polymer network [127,128]. Poly(ethylene glycol) methyl ether methacrylate(PEG/MA) and poly(ethylene glycol)-grafted graphene oxide (PEG/GO) as filler (0.2 wt.%) have demonstrated an excellent ionic conductivity of $2.1 \times 10^{-4}$ S/cm, boasting superior thermal and mechanical stabilities [129]. Wu et al. (2016) reported the PAN-based SPE (filled with 0.9 wt% GO nanosheets) increased the ionic conductivity ($1.1 \times 10^{-4}$ S/cm), and effectively improved the electrochemical stability [130].

By adding various fillers to polymers, the ionic conductivity of polymers can increase. This will decrease the melting point and will establish a good matrix-filler interaction in composites. It will also improve temperature and mechanical stabilities. Table 2 shows various types of inorganics as additives to improve polymer conductivity for SPEs fabrication. The incorporation of an inorganic filler to polymeric electrolytes can increase the ionic conductivity of the composite polymer electrolytes to between $10^{-5}$ and $10^{-2}$ S/cm. Composites based on gel electrolytes and zeolites have shown the highest conductivities (in the order of $10^{-2}$ S/cm). Capuano et al. (1991) concluded that filler loading and particle size were critical factors in effective improvement of ionic conductivity [162].

**Table 2** Various types of inorganics as additives to improve polymer conductivity for SPEs fabrication

| Polymer | Filler | Conductivity S/cm | Conduction stability voltage | Ref. |
|---------|--------|-------------------|------------------------------|------|
| PEO/PMMA | $TiO_2SiO_2$,$Al_2O_3$, $SnO_2$ | $10^{-5}$ | 3V | 131 |
| PEC | $TiO_2$ | $1.74 \times 10^{-4}$ | | 132 |
| PVDF-HFP | $TiO_2$ | $2 \times 10^{-3}$ | | 133 |
| PEO | $TiO_2$ | $2.11 \times 10^{-5}$ | 4V | 134 |
| PEGMEM/SMA | $TiO_2$ | $1.1 \times 10^{-4}$ | 5.4 V | 135 |
| PVDF-HFP/PMMA | $TiO_2$ | $2.49 \times 10^{-3}$ | 5V | 136 |
| PVA/PVDF | $TiO_2$,$SiO_2$ | $3.7 \times 10^{-3}$ ,$1.7 \times 10^{-4}$ | 5.6 V | 137 |
| PEO | $TiO_2$ | $2.62 \times 10^{-4}$ | | 138 |
| PVDF/PMMA | $TiO_2$ | $3.9 \times 10^{-3}$ | 5.1V | 139 |
| PMMA/MG49 | $TiO_2$-$ZrO_2$ | $1.2 \times 10^{-5}$ | | 140 |
| PVDF-HFP | N-doped $TiO_2$ | $6.7 \times 10^{-4}$ | | 141 |
| PAN/sulpholane | $TiO_2$-$SiO_2$ | $9.8 \times 10^{-4}$ | | 142 |

| PEO | TiO$_2$ | $4.9\times 10^{-5}$ | | 143 |
|---|---|---|---|---|
| PEO/EC | | $1.6\times10^{-4}$ | | |
| PVdF-HFP | TiO$_2$ | $1.11\times10^{-2}$ | | 144 |
| PVA-PVP | SiO$_2$ | $5.07\times10^{-6}$ | | 145 |
| PVDF-HFP/PE | SiO$_2$ | $1.03\times10^{-3}$ | 4.75V | 146 |
| PVDF-HFP/PEO | SiO$_2$ | $8.84\times10^{-3}$ | | 147 |
| PEO/ (TEOS) | SiO$_2$ | $4.4 \times 10^{-5}$ | 5.5V | 148 |
| PVA:PVDF | SiO$_2$ | $9.4\times10^{-4}$ | | 149 |
| PVDF/ EMIFSI | SiO$_2$ | $1.9\times10^{-3}$ | 2.8V | 150 |
| P(VDF-HFP) | SiO$_2$ | $1.08\times10^{-3}$ | 4.8V | 151 |
| PEO | Al$_2$O$_3$ | $1.5 \times 10^{-4}$ | | 152 |
| Polystyrene | Al$_2$O$_3$ | $9.78 \times 10^{-5}$ | | 153 |
| PVA/sodium acetate | Al$_2$O$_3$ | $1.05 \times 10^{-3}$ | | 154 |
| PEO | Al$_2$O$_3$ | $1.06 \times 10^{-5}$ | | 155 |
| PVdF-HFP | Al$_2$O$_3$ | $0.75\times 10^{-3}$ | | 156 |
| PVAc / PMMA | Al$_2$O$_3$ | $8.765\times 10^{-3}$ | | 157 |
| PVDF- HFP | GO | $1.04\times 10^{-3}$ | | 158 |
| PVA | GO | $31.6\times 10^{-3}$ | | 159 |
| PVA | GO | $29.21\times 10^{-3}$ | | 160 |
| PAN/LiClO$_4$ | GO | $4.03 \times 10^{-4}$ | | 161 |

Plasticizer, as additives with high dielectric constants and low viscosities, can be added to the host polymer. This can result in a drop in viscosity *via* the polymeric segmentation with weakened intramolecular forces between the polymer chains. This, consequently, reduces of the rigidity of the prepared films [163,164]. Plasticizers with relatively low molecular sizes can easily penetrate the space between the polymeric chains. This will minimize the prevalence of the secondary intermolecular attractive forces in polymer chains, hence an increase in free volume. This may well give rise to the segmental and charge-carrier mobilities. Low molecular weight polyglycols(PGs) are more common plasticizers. It was reported that the crystallinity phase of the polyethylene oxide (PEO) decreased after the addition of PGE200 as the plasticizer (PEG cross-linked with PEO segments), leading to the enhancement of the amorphous fraction in the film while increasing ionic conductivity to $10^{-4}$ S/cm [165]. The addition of plasticizers such as ethylene carbonate, polyethylene glycol [166], propylene carbonate [167], poly(vinylene carbonate)[168], dimethyl carbonate [169] to polymeric matrices has revealed considerable improvements in the ionic conductivity of SPEs due to a drop in the polymers'

Tg and an increase in salt dissolution and ionic transfer. The addition of polycarboxylate (PC) as plasticizer increased the PAN conductivity ($\sim10^{-2}$ S/cm). Plasticized systems are generally known for their poor mechanical stabilities, adversely limiting their commercial and technological applications.

Blending polymers has been suggested as an effective technique for reducing crystallinity and enhancing ion conductivity at room temperatures. High molecular weight crystalline and highly amorphous polymers are dissolved in common solvents to adjust ionic conductivity [170]. The polar groups in polymers could raise the dielectric constant of the polymeric blend. The polymer blends are associated with properties that are superior to the properties of individual polymers. However, the miscibility of homo-polymers on the molecular scale affects these superior properties. The polymers' blending method is easy to operate, while it provides a practical route to control the resultant physical properties *via* compositional changes. The polymer blends can be immiscible, compatible and miscible mixtures. PEO/PAN, PEO/PVC, PMMA/PVC, PMMA/P (VdF-HFP, PMMA/VAc, PVDF/PMMA, PVA/PVP, PAV/CMC, PVA/PAN, PPC/P(VdF-HFP) have been reported as effective polymer blends [171-173]. The most advantage of miscible polymer blends is the formation of a single-phase structure with a single glass transition temperature. PEO has a partial negative charge on its oxygen atoms and thus, acts as a proton acceptor to form miscible blends with a variety of proton-donating polymers [174]. Flexible hydrogel electrolytes can be prepared by blending bacterial cellulose with PVA. The blend demonstrated a nine-fold superior mechanical property [175].

The combination of polymers and ionic liquids can result in the growth of the amorphous phase, providing free volume and thus, facilitating ionic conduction. The use of several ionic liquids with cations based on imidazolium, pyrrolidium, piperidinium, morpholinium and quaternary ammonium in polymer electrolytes has been studied [176].

Significant improvements were observed in their ionic conductivities. Ammonium salts (good proton donors) such as $CH_3COONH_4$, $NH_4NO_3$, $NH_4Br$, $NH_4SCN$ [177] and inorganic acids such as $H_3PO_4$ [178] and $H_2SO_4$ [179] were also employed in the polymer matrices to increase the characteristic conductivities. Moreover, the presence of carbonyl groups (C=O) in side chains of polymers (*e.g.* PVA), enables free ionic mobility in polymer-salt systems. The addition of a dissolved polysulfide to liquid electrolytes or polymer electrolytes has been found to be the most promising in increasing the cell stability and efficiency. The sulfone- and sulfoxide-containing polymers have demonstrated improved cell performance due to the large size of the sulphur atom, which may also decrease the Tg of solid polymer electrolytes [180-183].

Several hypotheses have been proposed to explain the ionic conduction in solid electrolytes. Ionic conduction in solid electrolytes depends on several parameters e.g. presence of interstitial sites, crystal structure, ion size and temperature and etc. Generally, defects are divided into two groups - Schottky and Frenkel defects. Defects of crystal structures e.g. point-, planar-, line-, electron- and volume defects all may impact the ionic conductivity. Point defects of inorganic solid electrolytes (ISEs) are more pronounced in ion-transport mechanisms. Point defects are associated with the concentration and the type of the carriers. Ion sublattice, structure of immobile framework and spatial arrangement of immobile ions produce the crystal structure of ISEs. The interaction between immobile framework and metal-ions provides the remarkable effects on the metal-ion mobility, while the structures of immobile ions and spatial arrangements may affect metal-ion migration path. The defect chemistry of ISEs may explain the ion-transport mechanism. For Schottky defects, the metal (cation) ions should squeeze through the lattice, inducing significant distortion/relaxations. This, may in turn, limit the mobility of ions. The second key factor is the relatively high probability of ions which may jump to their original position, resulting in no net ionic

migration. In the other type defect (i.e. Frenkel defects), ions can migrate via two mechanisms e.g. direct interstitial jump and interstitialcy mechanism. For ion transfer in solid electrolytes, the systems should: (i) have available empty sites for ions to move through the lattice, (ii) have low activation energy barriers for electrons to jump between the neighbouring sites, (iii) have a solid framework, preferably a 3D one, permeable via open channels, (iiii) demonstrate highly polarizable framework ions (i.e. anions)[96,183,184].

## 5.2 Gel Polymer Electrolytes

Developing alternative polymer matrices at a low cost with wide electrochemical windows and devising simple synthetic methods are key factors in the development of high-performance batteries [150,184]. In order for polymeric electrolytes to compete with their liquid organic counterparts, they should demonstrate superior properties such as good ionic conductivities in the proximity of liquid electrolytes, high chemical, thermal and electrochemical stabilities (large potential windows) and high mechanical stabilities (*i.e.* to prevent short-circuits). The second category of electrolytes (*i.e.* gel polymer electrolyte) are characterized by a higher ambient ionic conductivity than SPEs [185]. They; however, exhibit lower mechanical properties. Gel polymer electrolytes (GPE) are known to be a transition between solid polymer and liquid electrolytes. GPEs consist of a solvent with a high ionic conductivity, encapsulated in the polymeric matrix with a good ionic conductivity ($10^{-4}$ to $10^{-3}$ S/cm) at ambient temperatures. GPEs can be produced by immobilizing organic solvents *e.g.* DME, diethyl carbonate (DEC), ethylene carbonate (EC), and 1,3-dioxolane (DOL) and etc. in a polymeric network. GPEs are more flexible compared to solid polymer electrolytes; they can be more readily scaled up and fabricated in various shapes. However, the mechanical strength of GPEs drops during the plasticizing process with organic solvents. Achieving high ionic conductivities, ensuring good contacts with the electrodes and good chemical and electrochemical stabilities are the major challenges in designing hydrogel networks. of the use

of an optimal polymer host, alkali salt and their optimised compositions have been reported to successfully address the mechanical strength of GPEs. The problems associated with low mechanical strengths can be rectified by combining inorganic solids (or other inorganic fillers) with host polymers to improve the mechanical strength. Porous structures in polymer matrices play an important role in GPEs as they are responsible for the uptake of liquid electrolytes [2,3,186]. However, it is worth mentioning that too large pores are detrimental for battery performance as they often induce internal short circuits.

PVA doped with KOH has been widely used as PGEs in various applications *e.g.* super-capacitors, anion exchange membranes, zinc batteries and fuel cells. (PGE) films, based on acrylate–KOH–$K_2S_2O_8$ have shown an ionic conductivity of 0.288 S/cm and good performance for application in zinc-air batteries [187]. Wu et al. 2006 studied the effects of KOH dosage in PVA matrices. In another study, the ionic conductivity was boosted to $47 \times 10^{-3}$ S/cm with a decrease in the mechanical stability of the polymer electrolyte [188]. PVA/PAA-KOH polymer electrolytes with an ionic conductivity between 0.142–0.301 S/cm (depending on the composition) exhibited a high utilisation percentage (*i.e.* 90%) in zn-air batteries [189]. GPE electrolytes based on PVA/KOH, exhibited good cycling stabilities for 6 and 12 hours in sandwich- and cable-type zinc air batteries, respectively [190,191]. However, low concentrations of KOH in GPEs (< 2 M) leads to a low ionic conductivity (*i.e.* $10^{-4} \sim 10^{-3}$ S/cm), and unsatisfied electrolyte uptake due to the close proximity of the cross-linked structures of the PVA matrix. Poor electrolyte retaining as a result of the half-opened system of ZABs with evaporation from the exposed air electrode side, also adversely impacts zinc air batteries [192]. PVA-KOH polymers, cross-linked with poly (ethylene glycol) diglycidyl ether, has shown an ionic conductivity of $2.2 \times 10^{-1}$ S/cm [193]. Polymerization of AM using N,N′-methylenebis (acrylamide) (MBAa) as cross-linker *via* UV light-initiated free radicals was done as PGEs with demonstrated good mechanical strengths and a high ionic conductivity (σ

= 0.33 S/cm ). The zinc-air battery performance indicated a stable voltage profile over 50 h of cycling with a power density of 39 mW/cm$^2$ [194]. Soaking PVA membranes in KOH solution (12 M) has improved the ionic conductivity to 0.34 S/cm. This was due to an increase in the PVA inter-chains canals, the enhancement of amorphosity in the host polymer, and H-bond network formation [185]. Tran et al. (2019) investigated three types of polymers (*i.e.* PVA, PAA and PAM) based on their chemical compositions and different charged functional groups in the polymer network [195]. The hydrogel network has impact on the electrolyte uptake and may influence the ionic conductivity. GPE based on PAA revealed the highest conductivity may be due to its high hydrophilicity as well. A cross-linked GPE, using PEO and PVA polymers (*i.e.* the host polymer) demonstrated a high ionic conductivity of 0.3 S/cm [196]. In order to increase the water retention capability of GPEs, several methods have been proposed to create and enhance the porous structure such as the addition of SiO$_2$ to PVA/PEG [197]. Fu et al. 2015 reported a flexible and rechargeable ZAB using porous polyvinyl alcohol (PVA) as the GPE. The porous GPE showed an outstanding stability over 120 cycles at a rate of 50 A/kg [198]. Xu et al. 2015 also reported a rechargeable, flexible and stretchable ZAB with a PVA/poly(ethylene oxide) (PEO)-based alkaline GPE. At the voltage plateau of 1.0 V, the discharge current density reached 1 A/g and was effectively maintained for 30 discharge/charge cycles [199]. In order to obtain gel polymer electrolyte with high water retention capability, Li et al. (2019) suggested the use of tetraethylammonium hydroxide (TEAOH) instead of KOH as the ionic conductor. Compared to KOH-PVA, a significant improvement in the shelf life of the TEAOH−PVA electrolyte was successfully achieved [200]. Gel polymer electrolytes demonstrate the ability to suppresses dendrite, owing to their uniform ionic flux distribution and single-ion transport (Schematic 4). Indeed, gel polymer electrolytes can mitigate the ion concentration gradient (i.e. the main key factor in dendrite growth). Also,

the intermolecular solvent channels can enhance the uniformity of current distribution, leading to homogenous zinc deposition.
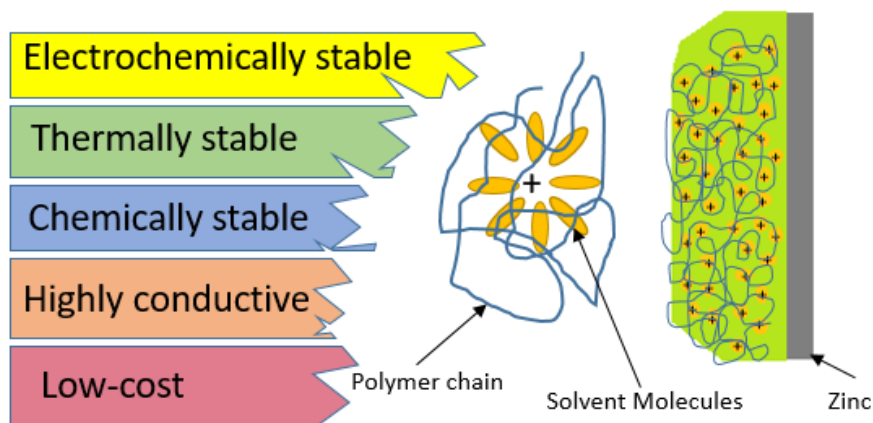


Schematic 3 The basic requirement aspects of gel polymers

## 6. Room Temperature Ionic Liquids (RTIL)

Ionic liquids (ILs) as molten salts have been studied more recently due to their decent electrochemical stability when compared to aqueous electrolytes. RTILs are composed of an organic cation (*i.e.* imidazolium cations ($RRIm^+$), pyridinium cations ($RRPy^+$), tetraalkylammonium cations ($RRRRN^+$)) combined with a variety of large anions having a delocalized charge (*i.e.* $PF_6^-$, $BF_4^-$, $N(F_2SO_2)_2^{2-}$). The main advantages of ILs over organic electrolytes are their low volatility, non-flammability, higher oxidation potential (~5.3 V) and their good thermal stability [2,3,197,201]. This would allow for enhanced reaction kinetics at higher temperatures without the any loss of electrolyte. The anions of ILs can coordinate with metal ions to form a new complex in order to manage the electrode/electrolyte interface behaviour. Moreover, the mitigation of zinc dendrite formation and zinc self-corrosion allows RTILs to extend the battery cycle life. However, main drawbacks are their relatively high viscosities and low ionic conductivities at low temperatures. In addition, formation of

superoxide ion ($O_2^{.-}$) as a strong nucleophile *via* the one-electron transfer pathway has a negative impact on $O_2$ redox reaction (ORR) kinetics [3,202-204].

Ionic liquids are highly tuneable materials which are typically classified into three types of protic, aprotic and zwitterionic based on how different cations and anions are paired. Pyrrolidinium-based ionic liquids show larger electrochemical stability potential windows (ESPWs) while imidazolium-based ionic liquids have better ionic conductivities [205]. The structural properties of RTILs are tuneable. This is often done *via* the incorporation of certain functional groups which can enhance the coordination of zinc ions in the electrolyte. This can, in turn, prevent the generation of undesirable by-products. Only few studies have been conducted on the use of ionic liquid-based electrolytes in zinc air batteries. In order to improve the ionic conductivity, an alternative strategy has been employed by combining ionic liquids with organic solvents to reduce viscosity while boosting the ionic mobility. Different behavioural patterns of zinc dendrites formation were observed upon adding imidazolium ILs (EMI) to electrolyte with various types of anion groups. EMI-Cl has shown the ability to form a loose deposit and contribute to minimise zinc dendrite formation. However, the use of EMI-$PF_6$ and EMI-TFSA has been linked to the establishment of a smooth deposit together with minimised dendrite growth. The addition of EMI-DCA extends the number of the active sites for dendrite initiation [206]. ILs based on oligo-ether side chains into a quaternary ammonium cation and bis (trifluoromethylsulfonyl) imide [NTf2] as the anion enhances the coordination and solubility of zinc ions and enhance the deposition and stripping reactions. ILs with the longer ether chain complexes stronger to the $Zn^{2+}$ ions [207]. Increasing the number of ether functional groups on cations leads to a drop in the melting point and the viscosity. However, modified RTILs show lower ionic conductivities. Zinc ions associated with ether oxygen atoms of the ammonium cation are associated with an increase in viscosity. The presence of water;

however, causes a decrease in viscosity [208]. Some ionic liquids such as1-methylimidazolium trifluoromethylsulfonate ([MIm]TfO) have can stabilise the zinc ions, while the *in situ* reduction of ZnO to Zn can make them promising electrolytes in rechargeable zinc–air batteries [209]. Dendritic growth of zinc was effectively minimised using $(Zn(TfO)^{2+} ZnO)/[EIm]TfO$ electrolyte. Both cationic $[Zn(EIm)2]^{2+}$ and anionic $[Zn(TfO)4]^{2-}$ complexes can effectively help to prevent dendritic growth [210].

The oxygen electrocatalysis in aqueous media is significantly different from that in aprotic electrolytes. The reversibility of the ORR/OER is a key issue for improving Zn-air batteries during the cyclic process. Various studies have reported on the influence of $H_2O$ on the ORR/OER, consequently affecting the electrochemical properties of Zn dissolving/deposition processes in Zn-air batteries. Air electrodes display different wettability in aprotic electrolytes. The viscous ionic liquids show a sharp voltage drop in zinc-air batteries using viscous ionic liquids as a result of the low wettability of gas-diffusion electrode. In spite of low wettability, the presence of metal cations affects the ORR/OER in aprotic organic electrolytes and RTILs. Small cations cause the irreversible reduction of $O_2$ gases which leads to insoluble metal peroxides or superoxides formation, whereas larger cations contribute to the reversible $O_2/O_2^-$ reactions [211]. The ORR in various types of RTILs does not contain $H^+$, therefore, the electron transfer in the ORR is quasi reversible:

$$O_2 + e^- \rightarrow O_2^{\cdot-} \tag{17}$$

It is not clear how reactive superoxide species is and whether it can maintain the stability for re-oxidizing back to $O_2$ gases during the operation of the battery. The stabilized superoxide radical has a tendency to re-oxidize during reverse potential sweep instead of reacting with other molecules due to ion-pairing interaction [212]. The columbic efficiency decreases due to the difference in diffusivity between the $O_2$ gas and the superoxide radicals, consequently, protonation and reduction reactions can partially become reversible. The OER leads to water

splitting during which 2 and 4 electrons may be released. It has been observed that the ability of some cations (RTILs) to associate with the water molecules during oxidation may correspond to more effective OER performance when compared to alkaline electrolytes [213]:

$$O_2^- + H^+ \rightarrow HO_2^{\cdot}$$

$$HO_2^{\cdot} + O_2^- \rightarrow O_2 + HO_2^-$$
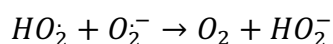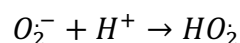
The reversibility of the 4-electron reduction has not yet been fully studied in RTILs. The conceptual pathways of proposed mechanisms have been described in Fig.12.
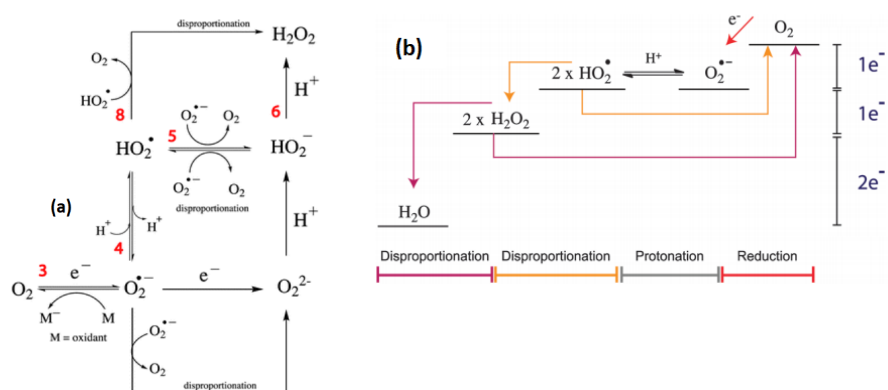


Fig. 12. (a) the steps involved in ORR in RTILs (b) the possible reactions involved in the 2-electron reduction of dioxygen to hydrogen peroxide[213].

## 7. Water-in-Salt Electrolytes

Water, as the electrolyte solvent, has a large dielectric constant, is inexpensive and non-toxic, has a small viscosity and is non-flammable. The development of aqueous electrolytes is limited due to the narrow electrochemical window of water (~1.23 V) which affects the performance of the cathode and anode materials. The narrow-electrochemical-window electrolytes are less energy-dense due to their dependency on the electrochemical potential window and capacity [214]:

$$E = CV$$

where, E, C and V are the energy density, capacity and operational electrochemical potential window of the battery. Novel electrolytes, "water-in-salt (WIS) or water-in-bi-salts", have been recently introduced with an aim to increase EPW (Figure 13). With salt being the dominant component, these electrolytes can improve the electrochemical potential window (EPW) of water to ~3 V. Non-flammability, electrochemical window potential (>2 V), low hydrogen evaluation and high ionic conductivity (>5 mS/cm) of water-in-salt electrolytes has gained a lot of attention for energy storages systems. WIS electrolytes are made up of dissolved salts in water solution in which the salt is the dominant species by both volume and mass. In WIS electrolytes, water molecules are coordinated with metal cations. In addition, the absence of free water molecules can prohibit corrosion at higher operating potentials.
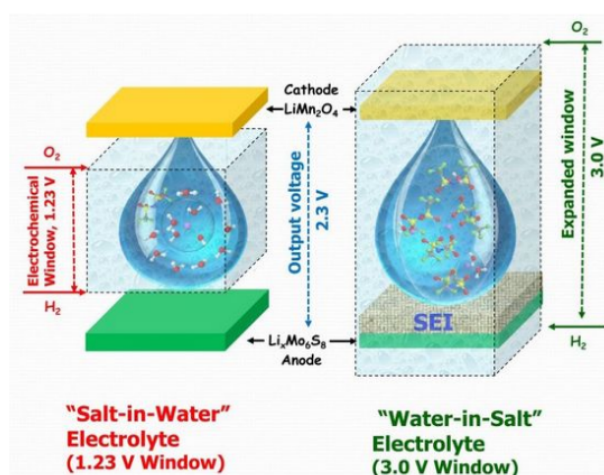


Figure 13: The electrochemical stability window of "water in salt" and "salt in water electrolytes" [215]

The free water molecules are less reactive than the $H_2O$ molecules in Lewis acid-base hydration shell, leading to suppressed reduction of water at the electrochemical interface due to the presence of hydrophilic cations (Schematic 5). The higher EPW of WIS electrolytes suggests the potential capability of these electrolytes to improve aqueous batteries, owing to stable cycling of high-potential cathode materials. Studies show that WIS electrolytes can be demonstrated in 4.0 V Li-ion batteries. Due to green, safer and longer cycling life, WIS

electrolytes are more suitable for sodium- and magnesium-ion batteries. Also, WIS electrolytes have been used to prepare supercapacitors. In WIS electrolytes, the solution is nearly saturated. This may cause undesirable salt crystallization in the cell which may lead to clogged pores, increased cell resistance and capacity loss [216].

The use of fluorinated salts e.g. bis(trifluoromethanesulfonyl)imide, lithium bis(trifluorosulfonimide), sodium bis(trifluorosulfonimide), sodium bis(fluorosulfonyl)imide, sodium trifluoromethanesulfonate and potassium tri-fluoromethanesulfonate has been recently studied in WIS electrolytes. However, fluorine content, changing pH and high costs have limited large-scale deployment. Inorganic salts, as alternatives to fluorinated salts, have been realised to be more efficient, are environmentally friendly and can be made at low costs; however, the process may lead to mechanical damage of the electrodes. Stabilizing the pH value using different hybrids (e.g. inorganic and fluorinated salts) is one of the efficient methods to enhance the energy density using water-in-bisalts e.g. of sodium acetate / sodium(I)bis(fluorosulfonyl)imide with a demonstrated EW of ~3.1 V.
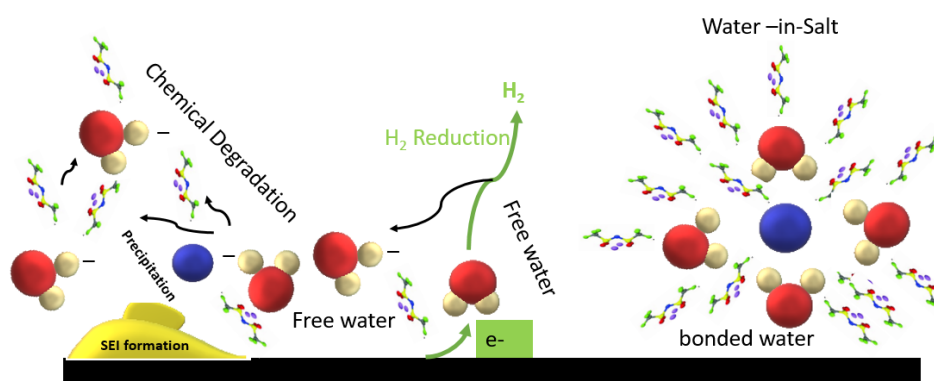


Schematic 5 Illustration of the evolution of the metal ion solvation both water-in-salt and dilute solutions

Ion transport processes and their role in the molecular/mesoscale structure of EIS electrolytes have been recently investigated. WIS electrolytes have been modelled to simulate

heterogeneous structures comprised of ions and water molecules, self-assembled in nanoscale domains with numerous ion-water interfaces. A 3D heterogeneous domain generates channels for the fast transport of hydrated metal ions, - a key parameter in high performance energy storage systems. WIS electrolytes comprise bulk and interfacial water molecules. The bulk water molecules are integrated with the ion network and act as a medium for ion transport (e.g. $Li^+$, $Na^+$). The interfacial water molecules act as lubricant (i.e. the conducting wire) and are dispersed in the porous 3D structure. Molecular dynamics simulation has predicted that the hydrated cation ions pass through the bulk water channels and are simultaneously lubricated by the interfacial water molecules. It was found that anions affect the structure of water and the stability of hydrogen bond. The demonstration of a higher electrochemical potential window depends on the structure of WIS electrolyte in the vicinity of the electrodes. Water molecules in WIS electrolytes are not free as the O-H bonds in the water molecules is reinforced, leading to reduced reactivity of the $H_2O$ molecules. Moreover, the transfer of electrons from the oxygen atom, linked to the metal-coordinated water molecule, to other ions results in the reduction of the highest occupied molecular orbital (HOMO) level and the enhancement of the oxidation potential of the $H_2O$ molecules. A WIS electrolyte consisting of Li-bis(trifluoromethane)sulphonamide (LiTFSI) and zinc salt, $Zn(TFSI)_2$, may improve the solvation structure of the $Zn^{2+}$ due to the high concentration of the TFSI anions. Wang et al. demonstrated reported that the formation of Zn metal was significantly suppressed, with a Coulombic efficiency of ~100%. Molecular dynamic simulations have also shown that the $Zn^{2+}$ ions may have a tendency to be surrounded by the TFSI anions instead of the free $H_2O$ molecules [216-218].

## 8. Conclusion

Zinc–air batteries suffer from poor cycle lives and energy efficiencies. These mainly originate from the adverse impacts of anode and cathode on recharge ability of these batteries.

Some of these issues are directly linked to the preferable liquid electrolytes (such as KOH), owing to their high ionic conductivities. In order to achieve better performance and cyclability, various studies have been reported on improving the anode's structure, replacing non-liquid electrolytes with suitable alternatives and synthesising efficient and novel catalysts. By improving liquid electrolytes and/or identifying more suitable non-aqueous alternative electrolytes, significant progress has been made to boost the ZABs' performance. There is; however, still a need to design new solid electrolytes with optimum ionic conductivities and mechanical strengths to enhance the lifetime as well as the batteries' energy efficiencies. In this review, we have reviewed and discussed the recent advances in the preparation and application of various (solid) electrolytes in the past few years. It has been unanimously agreed that adding efficient additives - in order to decrease zinc anode dissolution and consequently reducing structural change and dendrites formation - is an economical, yet straightforward method. However, little improvement was observed in the stability and the cyclability of ZABs. Neutral electrolytes, with no associated carbonate and dendrite formation, have been recognised as promising alternatives. However, the change in the electrolyte's pH and the slow rates of the ORR/OER are still limiting their widespread application in the field. Solid electrolytes based on polymer/ceramics are able to overcome some of these issues; however, in order to achieve the required ionic conductivities and appropriate mechanical strengths, more studies are deemed to be necessary.

## Acknowledgements

## References

[1] Schmitt, T, Arlt, T, Manke, I, Latz, A, & Horstmann, B Zinc electrode shape-change in secondary air batteries: A 2D modeling approach. Journal of Power Sources,2019:432:119-132.

[2] Deng, Ya-Ping, Yi Jiang, Ruilin Liang, Shao-Jian Zhang, Dan Luo, Yongfeng Hu, Xin Wang, Jun-Tao Li, Aiping Yu, and Zhongwei Chen. "Dynamic electrocatalyst with current-driven oxyhydroxide shell for rechargeable zinc-air battery." Nature Communications 11, no. 1 (2020): 1-10.

[3] Mainar, A. R., Iruin, E., Colmenares, L. C., Kvasha, A., de Meatza, I., Bengoechea, M., ... & Blazquez, J. A. An overview of progress in electrolytes for secondary zinc-air batteries and other storage systems based on zinc. Journal of Energy Storage, 2018;15: 304-328.

[4] Reddy, T. B. (2011). Linden's handbook of batteries (Vol. 4). New York: McGraw-hill.

[5] Sun, Y., Liu, X., Jiang, Y., Li, J., Ding, J., Hu, W., & Zhong, C. Recent advances and challenges in divalent and multivalent metal electrodes for metal–air batteries. Journal of Materials Chemistry A, 2019; 7(31):18183-18208.

[6] Gu, P., Zheng, M., Zhao, Q., Xiao, X., Xue, H., & Pang, H.. Rechargeable zinc–air batteries: a promising way to green energy. Journal of Materials Chemistry A, 2017; 5(17):7651-7666.

7] Alexander H. TULLO , C&EN NEW YORK CITY, Batteries that breathe air,;https://cen.acs.org/articles/95/i9/Batteries-breathe-air.html

[8] Garche, J., Dyer, C. K., Moseley, P. T., Ogumi, Z., Rand, D. A., & Scrosati, B. (Eds.). (2013). Encyclopedia of electrochemical power sources. Newnes.

[9] Zhang, J., Zhou, Q., Tang, Y., Zhang, L., & Li, Y. Zinc–air batteries: are they ready for prime time?. Chemical Science, 2019;10(39): 8924-8929.

[10]Stamm, J., Varzi, A., Latz, A., & Horstmann, B. Modeling nucleation and growth of zinc oxide during discharge of primary zinc-air batteries. Journal of Power Sources, 2017;360; 136-149.

[11] Fu, J., Cano, Z. P., Park, M. G., Yu, A., Fowler, M., & Chen, Z. Electrically rechargeable zinc–air batteries: progress, challenges, and perspectives. Advanced materials, 2017;29(7): 1604685.

[12] Deng, Y. P., Liang, R., Jiang, G., Jiang, Y., Yu, A., & Chen, Z. (2020). The Current State of Aqueous Zn-Based Rechargeable Batteries. ACS Energy Letters, 5(5), 1665-1675.

[13] Schröder, D., & Krewer, U. Model based quantification of air-composition impact on secondary zinc air batteries. Electrochimica Acta, 2014;117: 541-553.

[14] Li, Y., & Dai, H. Recent advances in zinc–air batteries. Chemical Society Reviews, 2014;43(15): 5257-5275.

[15] Popov, K. I., Živković, P. M., & Nikolić, N. Electrochemical aspects of formation of dendrites. Zaštita materijala, 2016;57(1); 55-62.

[16] Diggle, J. W., Despic, A. R., & Bockris, J. M. The mechanism of the dendritic electrocrystallization of zinc. Journal of The Electrochemical Society, 1969;116(11):1503-1514.

[17] Pei, A., Zheng, G., Shi, F., Li, Y., & Cui, Y. (2017). Nanoscale nucleation and growth of electrodeposited lithium metal. Nano letters, 17(2), 1132-1139.

[18] Guo, L., Guo, H., Huang, H., Tao, S., & Cheng, Y. (2020). Inhibition of zinc dendrites in zinc-based flow batteries. Frontiers in Chemistry, 8.

[19] Huang, C., Shi, R., Amini, A., Wu, Z., Xu, S., Zhang, L., ... & Wang, N. Hierarchical ZnO nanostructures with blooming flowers driven by screw dislocations. Scientific reports, 2015;5: 8226.

[20] Wang, R. Y., Kirk, D. W., & Zhang, G. X. Effects of deposition conditions on the morphology of zinc deposits from alkaline zincate solutions. Journal of The Electrochemical Society, 2006;153(5): C357-C364.

[21] Yufit, V., Tariq, F., Eastwood, D. S., Biton, M., Wu, B., Lee, P. D., & Brandon, N. P. Operando Visualization and Multi-scale Tomography Studies of Dendrite Formation and Dissolution in Zinc Batteries. Joule, 2019;3(2):485-502.

[22] Riede, J. C., Turek, T., & Kunz, U. (2018). Critical zinc ion concentration on the electrode surface determines dendritic zinc growth during charging a zinc air battery. Electrochimica Acta, 269, 217-224.

[23] Yufit, V., Tariq, F., Wu, B., Biton, M., Merla, Y., Eastwood, D., ... & Brandon, N. P. In-Operando X-ray Tomography Studies of Dendrite Formation in Zinc-Air Batteries. In Meeting Abstracts The Electrochemical Society 2014; 4: 229-229

[24]Biton, M., Tariq, F., Yufit, V., Chen, Z., & Brandon, N. Integrating multi-length scale high resolution 3D imaging and modelling in the characterisation and identification of mechanical failure sites in electrochemical dendrites. Acta Materialia, 2017;141: 39-46.

[25] Wang, K., Pei, P., Ma, Z., Chen, H., Xu, H., Chen, D., & Wang, X. (2015). Dendrite growth in the recharging process of zinc–air batteries. Journal of Materials Chemistry A, 3(45), 22648-22655.

[26] Cao, J., Zhang, D., Zhang, X., Sawangphruk, M., Qin, J., & Liu, R. (2020). A universal and facile approach to suppress dendrite formation for a Zn and Li metal anode. Journal of Materials Chemistry A, 8(18), 9331-9344.

[27] Yufit, V., Tariq, F., Eastwood, D. S., Biton, M., Wu, B., Lee, P. D., & Brandon, N. P. (2019). Operando visualization and multi-scale tomography studies of dendrite formation and dissolution in zinc batteries. Joule, 3(2), 485-502.

[28] Stock, D., Dongmo, S., Miyazaki, K., Abe, T., Janek, J., & Schröder, D. Towards zinc-oxygen batteries with enhanced cycling stability: The benefit of anion-exchange ionomer for zinc sponge anodes. Journal of Power Sources, 2018;395:195-204.

[29] Michlik, T., Schmid, M., Rosin, A., Gerdes, T., & Moos, R. Mechanical coating of zinc particles with Bi2O3-Li2O-ZnO glasses as anode material for rechargeable zinc-based batteries. Batteries, 2018;4(1):12.

[30] Wongrujipairoj, K., Poolnapol, L., Arpornwichanop, A., Suren, S., & Kheawhom, S. Suppression of zinc anode corrosion for printed flexible zinc-air battery. physica status solidi (b), 2017;254(2):1600442.

[31] Thomas, S., Cole, I. S., Sridhar, M., & Birbilis, N. (2013). Revisiting zinc passivation in alkaline solutions. Electrochimica Acta, 97, 192-201.

[32] Liu, M. B., Cook, G. M., & Yao, N. P. (1981). Passivation of zinc anodes in KOH electrolytes. Journal of the Electrochemical Society, 128(8), 1663-1668

[33] Sun, K. E., Hoang, T. K., Doan, T. N. L., Yu, Y., Zhu, X., Tian, Y., & Chen, P. Suppression of dendrite formation and corrosion on zinc anode of secondary aqueous batteries. ACS applied materials & interfaces, 2017;9(11), 9681-9687.

[34] The Nernst Equation and Pourbaix diagram, ' TLP Library, DoITPoMS, University of Cambridge, https://www.doitpoms.ac.uk/tlplib/pourbaix/index.php

[35] Park, J., Park, M., Nam, G., Lee, J. S., & Cho, J. (2015). All-solid-state cable-type flexible zinc–air battery. Advanced Materials, 27(8), 1396-1401.

[36] Hosseini, S., Han, S. J., Arponwichanop, A., Yonezawa, T., & Kheawhom, S. (2018). Ethanol as an electrolyte additive for alkaline zinc-air flow batteries. Scientific reports, 8(1), 11273.

[37] McLean, G. F., Niet, T., Prince-Richard, S., & Djilali, N. (2002). An assessment of alkaline fuel cell technology. International Journal of Hydrogen Energy, 27(5), 507-526.

[38] Huang, C. L., Wang, P. Y., & Li, Y. Y. (2020). Fabrication of electrospun CO2 adsorption membrane for zinc-air battery application. Chemical Engineering Journal, 125031.

[39] Xu, S., Das, S. K., & Archer, L. A. (2013). The Li–CO 2 battery: A novel method for CO 2 capture and utilization. RSC Advances, 3(18), 6656-6660.

[40] Jörissen, L. (2006). Bifunctional oxygen/air electrodes. Journal of Power Sources, 155(1), 23-32.

[41] Drillet, J. F., Holzer, F., Kallis, T., Müller, S., & Schmidt, V. M. (2001). Influence of CO2 on the stability of bifunctional oxygen electrodes for rechargeable zinc/air batteries and study of different CO 2 filter materials. Physical Chemistry Chemical Physics, 3(3), 368-371.

[42] Othman, R., Basirun, W. J., Yahaya, A. H., & Arof, A. K. (2001). Hydroponics gel as a new electrolyte gelling agent for alkaline zinc–air cells. Journal of power sources, 103(1), 34-41.

[43] Mohamad, A. A. (2006). Zn/gelled 6 M KOH/O2 zinc–air battery. Journal of power sources, 159(1), 752-757.

[44] Mitha, A., Mi, H., Dong, W., Cho, I. S., Ly, J., Yoo, S., ... & Chen, P. (2019). Thixotropic gel electrolyte containing poly (ethylene glycol) with high zinc ion concentration for the secondary aqueous Zn/LiMn2O4 battery. Journal of Electroanalytical Chemistry, 836, 1-6.

[45] Pal, B., Yang, S., Ramesh, S., Thangadurai, V., & Jose, R. (2019). Electrolyte selection for supercapacitive devices: a critical review. Nanoscale Advances, 1(10), 3807-3835.

[46] Xu, M., Ivey, D. G., Xie, Z., & Qu, W. (2015). Rechargeable Zn-air batteries: Progress in electrolyte development and cell configuration advancement. Journal of Power Sources, 283, 358-371.

[47] Khor, A., Leung, P., Mohamed, M. R., Flox, C., Xu, Q., An, L., ... & Shah, A. A. (2018). Review of zinc-based hybrid flow batteries: From fundamentals to applications. Materials today energy, 8, 80-108.

[48] Wei, X., Desai, D., Yadav, G. G., Turney, D. E., Couzis, A., & Banerjee, S. (2016). Impact of anode substrates on electrodeposited zinc over cycling in zinc-anode rechargeable alkaline batteries. Electrochimica Acta, 212, 603-613.

[49] Yi, J., Liang, P., Liu, X., Wu, K., Liu, Y., Wang, Y., ... & Zhang, J. (2018). Challenges, mitigation strategies and perspectives in development of zinc-electrode materials and fabrication for rechargeable zinc–air batteries. Energy & Environmental Science, 11(11), 3075-3095.

[50] Varzi, A., Raccichini, R., Passerini, S., & Scrosati, B. (2016). Challenges and prospects of the role of solid electrolytes in the revitalization of lithium metal batteries. Journal of Materials Chemistry A, 4(44), 17251-17259.

[51] Balbuena, P. B. (2014, June). Electrolyte materials-Issues and challenges. In AIP Conference Proceedings (Vol. 1597, No. 1, pp. 82-97). American Institute of Physics.

[52] Ortiz-Aparicio, J. L., Meas, Y., Trejo, G., Ortega, R., Chapman, T. W., & Chainet, E. (2013). Effects of organic additives on zinc electrodeposition from alkaline electrolytes. Journal of Applied Electrochemistry, 43(3), 289-300.

[53] Lee, C. W., Sathiyanarayanan, K., Eom, S. W., Kim, H. S., & Yun, M. S. (2006). Novel electrochemical behavior of zinc anodes in zinc/air batteries in the presence of additives. Journal of Power Sources, 159(2), 1474-1477.

[54] Nartey, V. K., Binder, L., & Kordesch, K. (1994). Identification of organic corrosion inhibitors suitable for use in rechargeable alkaline zinc batteries. Journal of power sources, 52(2), 217-222.

[55] Youssef, K. M., Koch, C. C., & Fedkiw, P. S. (2004). Influence of additives and pulse electrodeposition parameters on production of nanocrystalline zinc from zinc chloride electrolytes. Journal of The Electrochemical Society, 151(2), C103-C111.

[56] Hosseini, S., Abbasi, A., Uginet, L. O., Haustraete, N., Praserthdam, S., Yonezawa, T., & Kheawhom, S. (2019). The Influence of Dimethyl Sulfoxide as Electrolyte Additive on Anodic Dissolution of Alkaline Zinc-Air Flow Battery. Scientific Reports, 9(1), 1-12.

[57] Lan, C. J., Lee, C. Y., & Chin, T. S. (2007). Tetra-alkyl ammonium hydroxides as inhibitors of Zn dendrite in Zn-based secondary batteries. Electrochimica acta, 52(17), 5407-5416.

[58] Ein-Eli, Y., Auinat, M., & Starosvetsky, D. (2003). Electrochemical and surface studies of zinc in alkaline solutions containing organic corrosion inhibitors. Journal of power sources, 114(2), 330-337.

[59] Banik, S. J., & Akolkar, R. (2015). Suppressing dendritic growth during alkaline zinc electrodeposition using polyethylenimine additive. Electrochimica Acta, 179, 475-481.

[60] Zhou, D., Shanmukaraj, D., Tkacheva, A., Armand, M., & Wang, G. (2019). Polymer electrolytes for lithium-based batteries: advances and prospects. Chem, 5(9), 2326-2352.

[61] Lan, C. J., Lee, C. Y., & Chin, T. S. (2007). Tetra-alkyl ammonium hydroxides as inhibitors of Zn dendrite in Zn-based secondary batteries. Electrochimica acta, 52(17), 5407-5416.

[62] Ding, M. S., von Cresce, A., & Xu, K. (2017). Conductivity, viscosity, and their correlation of a super-concentrated aqueous electrolyte. The Journal of Physical Chemistry C, 121(4), 2149-2153.

[63] Yang, H., Cao, Y., Ai, X., & Xiao, L. (2004). Improved discharge capacity and suppressed surface passivation of zinc anode in dilute alkaline solution using surfactant additives. Journal of Power Sources, 128(1), 97-101.

[64] Kan, J., Xue, H., & Mu, S. (1998). Effect of inhibitors on Zn-dendrite formation for zinc-polyaniline secondary battery. Journal of Power Sources, 74(1), 113-116.

[65] Sun, K. E., Hoang, T. K., Doan, T. N. L., Yu, Y., Zhu, X., Tian, Y., & Chen, P. (2017). Suppression of dendrite formation and corrosion on zinc anode of secondary aqueous batteries. ACS applied materials & interfaces, 9(11), 9681-9687.

[66] Liu, K., He, P., Bai, H., Chen, J., Dong, F., Wang, S., ... & Yuan, S. (2017). Effects of dodecyltrimethylammonium bromide surfactant on both corrosion and passivation behaviors of zinc electrodes in alkaline solution. Materials Chemistry and Physics, 199, 73-78.

[67] Hosseini, S., Lao-Atiman, W., Han, S. J., Arpornwichanop, A., Yonezawa, T., & Kheawhom, S. (2018). Discharge Performance of Zinc-Air Flow Batteries Under the Effects of Sodium Dodecyl Sulfate and Pluronic F-127. Scientific reports, 8(1), 14909.

[68] Ghavami, R. K., Rafiei, Z., & Tabatabaei, S. M. (2007). Effects of cationic CTAB and anionic SDBS surfactants on the performance of Zn–MnO2 alkaline batteries. Journal of Power Sources, 164(2), 934-946.

[69] Ghavami, R. K., Kameli, F., Shirojan, A., & Azizi, A. (2016). Effects of surfactants on sulfation of negative active material in lead acid battery under PSOC condition. Journal of Energy Storage, 7, 121-130.

[70] Vatsalarani, J., Trivedi, D. C., Ragavendran, K., & Warrier, P. C. (2005). Effect of polyaniline coating on "shape change" phenomenon of porous zinc electrode. Journal of the Electrochemical Society, 152(10), A1974-A1978.

[71] Vatsalarani, J., Geetha, S., Trivedi, D. C., & Warrier, P. C. (2006). Stabilization of zinc electrodes with a conducting polymer. Journal of power sources, 158(2), 1484-1489.

[72] Zhang, C., Wang, J. M., Zhang, L., Zhang, J. Q., & Cao, C. N. (2001). Study of the performance of secondary alkaline pasted zinc electrodes. Journal of applied electrochemistry, 31(9), 1049-1054.

[73] Lee, C. W., Sathiyanarayanan, K., Eom, S. W., & Yun, M. S. (2006). Novel alloys to improve the electrochemical behavior of zinc anodes for zinc/air battery. Journal of power sources, 160(2), 1436-1441.

[74] Jo, Y. N., Kim, H. S., Prasanna, K., Ilango, P. R., Lee, W. J., Eom, S. W., & Lee, C. W. (2014). Effect of additives on electrochemical and corrosion behavior of gel type electrodes for Zn-air system. Industrial & Engineering Chemistry Research, 53(44), 17370-17375.

[75] Jo, Y. N., Kang, S. H., Prasanna, K., Eom, S. W., & Lee, C. W. (2017). Shield effect of polyaniline between zinc active material and aqueous electrolyte in zinc-air batteries. *Applied Surface Science*, *422*, 406-412.

[76] Stock, D., Dongmo, S., Damtew, D., Stumpp, M., Konovalova, A., Henkensmeier, D., ... & Schröder, D. (2018). Design Strategy for Zinc Anodes with Enhanced Utilization and Retention: Electrodeposited Zinc Oxide on Carbon Mesh Protected by Ionomeric Layers. *ACS Applied Energy Materials*, *1*(10), 5579-5588.

[77] Clark, S., Latz, A., & Horstmann, B. (2017). Rational development of neutral aqueous electrolytes for zinc–air batteries. *ChemSusChem*, *10*(23), 4735-4747.

[78] Sumboja, A., Ge, X., Zheng, G., Goh, F. T., Hor, T. A., Zong, Y., & Liu, Z. (2016). Durable rechargeable zinc-air batteries with neutral electrolyte and manganese oxide catalyst. *Journal of Power Sources*, *332*, 330-336.

[79] Goh, F. T., Liu, Z., Hor, T. A., Zhang, J., Ge, X., Zong, Y., ... & Khoo, W. (2014). A near-neutral chloride electrolyte for electrically rechargeable zinc-air batteries. *Journal of The Electrochemical Society*, *161*(14), A2080-A2086.

[80] Sumboja, A., Ge, X., Zheng, G., Goh, F. T., Hor, T. A., Zong, Y., & Liu, Z. (2016). Durable rechargeable zinc-air batteries with neutral electrolyte and manganese oxide catalyst. Journal of Power Sources, 332, 330-336.

[81] Amendola, S., Binder, M., Black, P. J., Sharp-Goldman, S., Johnson, L., Kunz, M., ... & Johnson, R. (2012). *U.S. Patent Application No. 12/841,115*.

[82] Vos, J. G., & Koper, M. T. M. (2018). Measurement of competition between oxygen evolution and chlorine evolution using rotating ring-disk electrode voltammetry. Journal of Electroanalytical Chemistry, 819, 260-268.

[83] Zhao, S., An, H., & Chen, S. (1998). A study of a high-power, ammonium chloride zinc/manganese dioxide dry battery. Journal of power sources, 76(2), 218-220.

[84] Jindra, J., Mrha, J., & Musilová, M. (1973). Zinc-air cell with neutral electrolyte. Journal of Applied Electrochemistry, 3(4), 297-301.

[85] Goh, F. T., Liu, Z., Hor, T. A., Zhang, J., Ge, X., Zong, Y., ... & Khoo, W. (2014). A near-neutral chloride electrolyte for electrically rechargeable zinc-air batteries. Journal of The Electrochemical Society, 161(14), A2080-A2086.

[86] Liu, S., Han, W., Cui, B., Liu, X., Zhao, F., Stuart, J., & Licht, S. (2017). A novel rechargeable zinc-air battery with molten salt electrolyte. *Journal of Power Sources*, *342*, 435-441.

[87] Fan, L., Wei, S., Li, S., Li, Q., & Lu, Y. (2018). Recent progress of the solid-state electrolytes for high-energy metal-based batteries. *Advanced Energy Materials*, *8*(11), 1702657.

[88] Zhang, W., Tu, Z., Qian, J., Choudhury, S., Archer, L. A., & Lu, Y. (2018). Design Principles of Functional Polymer Separators for High-Energy, Metal-Based Batteries. *Small*, *14*(11), 1703001.

[89] Cheng, X., Pan, J., Zhao, Y., Liao, M., & Peng, H. (2018). Gel polymer electrolytes for electrochemical energy storage. *Advanced Energy Materials*, *8*(7), 1702184..

[90] Aziz, S. B., Woo, T. J., Kadir, M. F. Z., & Ahmed, H. M. (2018). A conceptual review on polymer electrolytes and ion transport models. Journal of Science: Advanced Materials and Devices, 3(1), 1-17.

[91] Chen, S., Wen, K., Fan, J., Bando, Y., & Golberg, D. (2018). Progress and future prospects of high-voltage and high-safety electrolytes in advanced lithium batteries: from liquid to solid electrolytes. Journal of Materials Chemistry A, 6(25), 11631-11663.

[92] Wu, F., Fitzhugh, W., Ye, L., Ning, J., & Li, X. (2018). Advanced sulfide solid electrolyte by core-shell structural design. Nature communications, 9(1), 4037.

[93] Kamaya, N., Homma, K., Yamakawa, Y., Hirayama, M., Kanno, R., Yonemura, M., ... & Mitsui, A. (2011). A lithium superionic conductor. Nature materials, 10(9), 682.

[94] Mizuno, F., Hayashi, A., Tadanaga, K., & Tatsumisago, M. (2005). New, highly ion-conductive crystals precipitated from Li2S–P2S5 glasses. Advanced Materials, 17(7), 918-921.

[95] Jung, Y. C., Lee, S. M., Choi, J. H., Jang, S. S., & Kim, D. W. (2015). All solid-state lithium batteries assembled with hybrid solid electrolytes. Journal of The Electrochemical Society, 162(4), A704-A710.

[96] Chen, M., Feng, G., & Qiao, R. (2020). Water-in-salt electrolytes: An interfacial perspective. Current Opinion in Colloid & Interface Science, 47, 99-110.

[97] Gao, H., & Lian, K. (2014). Proton-conducting polymer electrolytes and their applications in solid supercapacitors: a review. RSC Advances, 4(62), 33091-33113.

[98] Rivas, B. L., Pereira, E. D., & Moreno-Villoslada, I. (2003). Water-soluble polymer–metal ion interactions. Progress in Polymer Science, 28(2), 173-208.

[99] Aurbach, D., Zinigrad, E., Cohen, Y., & Teller, H. (2002). A short review of failure mechanisms of lithium metal and lithiated graphite anodes in liquid electrolyte solutions. Solid state ionics, *148*(3-4), 405-416.

[100] Wang, A., Kadam, S., Li, H., Shi, S., & Qi, Y. (2018). Review on modeling of the anode solid electrolyte interphase (SEI) for lithium-ion batteries. npj Computational Materials, 4(1), 15.

[101] Hamidah, N. L., Wang, F. M., & Nugroho, G. (2019). The understanding of solid electrolyte interface (SEI) formation and mechanism as the effect of flouro-o-phenylenedimaleimaide (F-MI) additive on lithium-ion battery. Surface and Interface Analysis, 51(3), 345-352.

[102] Manthiram, A., Yu, X., & Wang, S. (2017). Lithium battery chemistries enabled by solid-state electrolytes. Nature Reviews Materials, 2(4), 16103.

[103] Yang, J., Wang, X., Zhang, G., Ma, A., Chen, W., Shao, L., ... & Xie, K. (2019). High-performance solid composite polymer electrolyte for all solid-sate lithium battery through facile microstructure regulation. Frontiers in Chemistry, 7, 388.

[104] Fan, L., Wei, S., Li, S., Li, Q., and Lu, Y. (2018). Recent progress of the solid-state electrolytes for high-energy metal-based batteries. Adv. Energy Mater. 8:1702657. doi: 10.1002/aenm.201702657

[105] Ban, X., Zhang, W., Chen, N., and Sun, C. (2018). A high-performance and durable poly(ethylene oxide)-based composite solid electrolyte for all solid-state lithium battery. J. Phys. Chem. C 122, 9852–9858. doi: 10.1021/acs.jpcc.8b02556

[106] Thomas, K. E., Sloop, S. E., Kerr, J. B., & Newman, J. (2000). Comparison of lithium-polymer cell performance with unity and nonunity transference numbers. Journal of Power Sources, 89(2), 132-138.

[107] Tadros, T. F. (2015). Interfacial phenomena and colloid stability: basic principles (Vol. 1). Walter de Gruyter GmbH & Co KG.

[108] http://polymerdatabase.com/home.html

[109] Chen, F., Zha, W., Yang, D., Cao, S., Shen, Q., Zhang, L., & Sadoway, D. R. (2018). All-Solid-State Lithium Battery Fitted with Polymer Electrolyte Enhanced by Solid Plasticizer and Conductive Ceramic Filler. Journal of The Electrochemical Society, 165(14), A3558-A3565.

[110] Liu, W., Liu, N., Sun, J., Hsu, P. C., Li, Y., Lee, H. W., & Cui, Y. (2015). Ionic conductivity enhancement of polymer electrolytes with ceramic nanowire fillers. Nano letters, 15(4), 2740-2745.

[111] Wu, J. F., & Guo, X. (2019). MOF-derived nanoporous multifunctional fillers enhancing the performances of polymer electrolytes for solid-state lithium batteries. Journal of Materials Chemistry A, 7(6), 2653-2659.

[112] Thakur, A. K., & Hashmi, S. A. (2010). Polymer matrix–filler interaction mechanism for modified ion transport and glass transition temperature in the polymer electrolyte composites. Solid State Ionics, 181(27-28), 1270-1278.

[113] Gavrilov, A. A., Chertovich, A. V., Khalatur, P. G., & Khokhlov, A. R. (2014). Study of the mechanisms of filler reinforcement in elastomer nanocomposites. Macromolecules, 47(15), 5400-5408.

[114] Rahman, M. Y. A., Ahmad, A., Ismail, L. H. C., & Salleh, M. M. (2010). Fabrication and characterization of a solid polymeric electrolyte of PAN-TiO2-LiClO4. Journal of applied polymer science, 115(4), 2144-2148.

[115] Kurc, B. (2014). Precipitated silica as filler for polymer electrolyte based on poly (acrylonitrile)/sulfolane. Journal of Solid State Electrochemistry, 18(7), 2035-2046.

[116] Taherian, R., & Kausar, A. (2018). Electrical Conductivity in Polymer-Based Composites: Experiments, Modelling, and Applications. William Andrew.

[117] Ji, K. S., Moon, H. S., Kim, J. W., & Park, J. W. (2003). Role of functional nano-sized inorganic fillers in poly (ethylene) oxide-based polymer electrolytes. Journal of Power Sources, 117(1-2), 124-130.

[118] Zou, H., Wu, S., & Shen, J. (2008). Polymer/silica nanocomposites: preparation, characterization, properties, and applications. *Chemical reviews*, *108*(9), 3893-3957.

[119] Choi, J. H., Lee, C. H., Yu, J. H., Doh, C. H., & Lee, S. M. (2015). Enhancement of ionic conductivity of composite membranes for all-solid-state lithium rechargeable batteries incorporating tetragonal Li7La3Zr2O12 into a polyethylene oxide matrix. *Journal of Power Sources*, *274*, 458-463.

[120] Jiang, G., Maeda, S., Saito, Y., Tanase, S., & Sakai, T. (2005). Ceramic-polymer electrolytes for all-solid-state lithium rechargeable batteries. Journal of The Electrochemical Society, 152(4), A767-A773.

[121] Das, S., & Ghosh, A. (2015). Ion conduction and relaxation in PEO-LiTFSI-Al2O3 polymer nanocomposite electrolytes. *Journal of Applied Physics*, *117*(17), 174103.

[122] Croce, F., Persi, L., Scrosati, B., Serraino-Fiory, F., Plichta, E., & Hendrickson, M. A. (2001). Role of the ceramic fillers in enhancing the transport properties of composite polymer electrolytes. *Electrochimica Acta*, *46*(16), 2457-2461.

[123] Jayathilaka, P. A. R. D., Dissanayake, M. A. K. L., Albinsson, I., & Mellander, B. E. (2002). Effect of nano-porous Al2O3 on thermal, dielectric and transport properties of the (PEO) 9LiTFSI polymer electrolyte system. *Electrochimica acta*, *47*(20), 3257-3268.

[124] Egashira, M., Utsunomiya, Y., Yoshimoto, N., & Morita, M. (2006). Effects of the surface treatment of the $Al_2O_3$ filler on the lithium electrode/solid polymer electrolyte interface properties. Electrochimica acta, 52(3), 1082-1086.

[125] Dissanayake, M. A. K. L., Jayathilaka, P. A. R. D., Bokalawala, R. S. P., Albinsson, I., & Mellander, B. E. (2003). Effect of concentration and grain size of alumina filler on the ionic conductivity enhancement of the (PEO) $9LiCF_3SO_3$: $Al_2O_3$ composite polymer electrolyte. Journal of Power Sources, 119, 409-414.

[126] Prajapati, G. K., & Gupta, P. N. (2011). Comparative study of the electrical and dielectric properties of PVA–PEG–$Al_2O_3$–MI (M= Na, K, Ag) complex polymer electrolytes. Physica B: Condensed Matter, 406(15-16), 3108-3113.

[127] Korkmaz, S., & Kariper, İ. A. (2020). Graphene and graphene oxide based aerogels: Synthesis, characteristics and supercapacitor applications. *Journal of Energy Storage*, *27*, 101038.

[128] Vargas-Hernández, M. Á., Sulbarán-Rangel, B., & Vázquez-Torres, H. (2020). Non-isothermal curing kinetics of biocomposite from poly (furfuryl alcohol) and graphene oxide or reduced graphene oxide with different contents of oxygen-groups by DSC. Thermochimica Acta, *684*, 178485.

[129] Shim, J., Kim, D. G., Kim, H. J., Lee, J. H., Baik, J. H., & Lee, J. C. (2014). Novel composite polymer electrolytes containing poly (ethylene glycol)-grafted graphene oxide for all-solid-state lithium-ion battery applications. Journal of Materials Chemistry *A*, *2*(34), 13873-13883.

[130] Wu, B., Wang, L., Li, Z., Zhao, M., Chen, K., Liu, S., ... & Li, J. (2016). Performance of "polymer-in-salt" electrolyte PAN-LiTFSI enhanced by graphene oxide filler. Journal of The Electrochemical Society, *163*(10), A2248-A2252.

[131] Dhatarwal, P., Choudhary, S., & Sengwa, R. J. (2018). Electrochemical performance of Li+-ion conducting solid polymer electrolytes based on PEO–PMMA blend matrix incorporated with various inorganic nanoparticles for the lithium ion batteries. Composites Communications, *10*, 11-17.

[132] Pignanelli, F., Romero, M., Castiglioni, J., Faccio, R., & Mombrú, A. W. (2019). Novel synergistic in situ synthesis of lithium-ion poly (ethylene citrate)-TiO2 nanocomposites as promising fluorine-free solid polymer electrolytes for lithium batteries. Journal of Physics and Chemistry of Solids, *135*, 109082

[133] Zhai, W., Zhang, Y. W., Wang, L., Cai, F., Liu, X. M., Shi, Y. J., & Yang, H. (2016). Study of nano-TiO2 composite polymer electrolyte incorporating ionic liquid PP12O1TFSI for lithium battery. Solid State Ionics, *286*, 111-116.

[134] Polu, A. R., & Rhee, H. W. (2016). Effect of TiO2 nanoparticles on structural, thermal, mechanical and ionic conductivity studies of PEO12–LiTDI solid polymer electrolyte. Journal of Industrial and Engineering Chemistry, *37*, 347-353.

[135] Ma, C., Zhang, J., Xu, M., Xia, Q., Liu, J., Zhao, S., ... & Wei, W. (2016). Cross-linked branching nanohybrid polymer electrolyte with monodispersed TiO2 nanoparticles for high performance lithium-ion batteries. Journal of Power Sources, *317*, 103-111.

[136] Song, D., Xu, C., Chen, Y., He, J., Zhao, Y., Li, P., ... & Fu, F. (2015). Enhanced thermal and electrochemical properties of PVDF-HFP/PMMA polymer electrolyte by TiO2 nanoparticles. *Solid State Ionics*, *282*, 31-36

[137] Hema, M., & Tamilselvi, P. (2016). Lithium ion conducting PVA: PVdF polymer electrolytes doped with nano SiO2 and TiO2 filler. Journal of Physics and Chemistry of Solids, *96*, 42-48.

[138] Nimah, Y. L., Cheng, M. Y., Cheng, J. H., Rick, J., & Hwang, B. J. (2015). Solid-state polymer nanocomposite electrolyte of TiO2/PEO/NaClO4 for sodium ion batteries. Journal of Power Sources, *278*, 375-381.

[139] Zhou, L., Wu, N., Cao, Q., Jing, B., Wang, X., Wang, Q., & Kuang, H. (2013). A novel electrospun PVDF/PMMA gel polymer electrolyte with in situ TiO2 for Li-ion batteries. Solid State Ionics, *249*, 93-97.

[140] TianKhoon, L., Hassan, N. H., Rahman, M. Y. A., Vedarajan, R., Matsumi, N., & Ahmad, A. (2015). One-pot synthesis nano-hybrid ZrO2–TiO2 fillers in 49% poly (methyl methacrylate) grafted natural rubber (MG49) based nano-composite polymer electrolyte for lithium ion battery application. *Solid State Ionics*, *276*, 72-79.

[141] Kim, K. S., & Park, S. J. (2012). Influence of N-doped TiO2 on lithium ion conductivity of porous polymeric electrolyte membrane containing LiClO4. *Solid State Ionics*, *212*, 18-25.

[142] Kurc, B. (2014). Gel electrolytes based on poly (acrylonitrile)/sulpholane with hybrid TiO2/SiO2 filler for advanced lithium polymer batteries. Electrochimica Acta, *125*, 415-420.

[143] Vgnairooban, K., Dissanayake, M. A. K. L., Albinsson, I., & Mellander, B. E. (2014). Effect of TiO2 nano-filler and EC plasticizer on electrical and thermal properties of poly (ethylene oxide)(PEO) based solid polymer electrolytes. Solid State Ionics, *266*, 25-28.

[144] Kumar, P. S., Sakunthala, A., Govindan, K., Reddy, M. V., & Prabu, M. (2016). Single crystalline TiO 2 nanorods as effective fillers for lithium ion conducting PVdF-HFP based composite polymer electrolytes. RSC advances, 6(94), 91711-91719.

[145] Singh, P., Gupta, P. N., & Saroj, A. L. (2019). Ion dynamics and dielectric relaxation behavior of PVA-PVP-NaI-SiO2 based nano-composites polymer blend electrolytes. *Physica B: Condensed Matter*, 411850.

[146] Wu, J., Zuo, X., Chen, Q., Deng, X., Liang, H., Zhu, T., Nan, J. (2019). Functional composite polymer electrolytes with imidazole modified SiO2 nanoparticles for high-voltage cathode lithium ion batteries. *Electrochimica Acta*, *320*, 134567.

[147] Zebardastan, N., Khanmirzaei, M. H., Ramesh, S., & Ramesh, K. (2016). Novel poly (vinylidene fluoride-co-hexafluoro propylene)/polyethylene oxide based gel polymer electrolyte containing fumed silica (SiO2) nanofiller for high performance dye-sensitized solar cell. *Electrochimica Acta*, *220*, 573-580.

[148]Lin, D., Liu, W., Liu, Y., Lee, H. R., Hsu, P. C., Liu, K., & Cui, Y. (2015). High ionic conductivity of composite solid polymer electrolyte via in situ synthesis of monodispersed SiO2 nanospheres in poly (ethylene oxide). *Nano letters*, *16*(1), 459-465.

[149] Hema, M., Tamilselvi, P., & Pandaram, P. (2017). Conductivity enhancement in SiO2 doped PVA: PVDF nanocomposite polymer electrolyte by gamma ray irradiation. *Nuclear Instruments and Methods in Physics Research Section B: Beam Interactions with Materials and Atoms*, *403*, 13-20.

[150] Ortega, P. F., Trigueiro, J. P. C., Silva, G. G., & Lavall, R. L. (2016). Improving supercapacitor capacitance by using a novel gel nanocomposite polymer electrolyte based on nanostructured SiO2, PVDF and imidazolium ionic liquid. *Electrochimica Acta*, *188*, 809-817.

[151] Zhang, P., Yang, L. C., Li, L. L., Ding, M. L., Wu, Y. P., & Holze, R. (2011). Enhanced electrochemical and mechanical properties of P (VDF-HFP)-based composite polymer electrolytes with SiO2 nanowires. *Journal of membrane science*, *379*(1-2), 80-85.

[152] Pitawala, H. M. J. C., Dissanayake, M. A. K. L., & Seneviratne, V. A. (2007). Combined effect of Al2O3 nano-fillers and EC plasticizer on ionic conductivity enhancement in the solid polymer electrolyte (PEO) 9LiTf. *Solid State Ionics*, *178*(13-14), 885-888.

[153] Lim, Y. J., An, Y. H., & Jo, N. J. (2012). Polystyrene-Al 2 O 3 composite solid polymer electrolyte for lithium secondary battery. Nanoscale research letters, 7(1), 19.

[154] Kumar, M. S., & Rao, M. C. (2019). Effect of Al2O3 on structural and dielectric properties of PVP-CH3COONa based solid polymer electrolyte films for energy storage devices. *Heliyon*, *5*(10), e02727.

[155] Yap, Y. L., Cheang, P. L., You, A. H., & Teo, L. L. (2015). Modelling of temperature dependence on PEO electrolyte with Al2O3. Computational Materials Science, 106, 59-63.

[156]Yang, Y., Huang, X., Cao, Z., & Chen, G. (2016). Thermally conductive separator with hierarchical nano/microstructures for improving thermal management of batteries. Nano energy, 22, 301-309.

[157] Pradeepa, P., Sowmya, G., Edwinraj, S., Begum, G. F., & Prabhu, M. R. (2016). Influence of Al2O3 on the structure and electrochemical properties of PVAc/PMMA based blend composite polymer electrolytes. Materials Today: Proceedings, 3(6), 2187-2196.

[158] Ahmad, A. L., Farooqui, U. R., & Hamid, N. A. (2018). Effect of graphene oxide (GO) on Poly (vinylidene fluoride-hexafluoropropylene)(PVDF-HFP) polymer electrolyte membrane. Polymer, 142, 330-336.

[159] Wang, J., Chen, H., Ma, Y., Bai, H., Shi, B., Hou, C., Li, Y. (2020). Grafting high content of imidazolium polymer brushes on graphene oxide for nanocomposite membranes with enhanced anion transport. Reactive and Functional Polymers, 146, 104447.

[160] Alipoori, S., Torkzadeh, M. M., Moghadam, M. M., Mazinani, S., Aboutalebi, S. H., & Sharif, F. (2019). Graphene oxide: An effective ionic conductivity promoter for phosphoric acid-doped poly (vinyl alcohol) gel electrolytes. Polymer, 184, 121908.

[161] Jia, W., Li, Z., Wu, Z., Wang, L., Wu, B., Wang, Y., Li, J. (2018). Graphene oxide as a filler to improve the performance of PAN-LiClO4 flexible solid polymer electrolyte. Solid State Ionics, 315, 7-13.

[162] Capuano, F., Croce, F., & Scrosati, B. (1991). Composite polymer electrolytes. *Journal of the Electrochemical Society*, *138*(7), 1918-1922.

[163] Honary, S., & Orafai, H. (2002). The effect of different plasticizer molecular weights and concentrations on mechanical and thermomechanical properties of free films. *Drug development and industrial pharmacy*, *28*(6), 711-715.

[164] Honari, S., & Golkar , M. (2003). Effect of polymer grade and plasticizer molecular weights on viscoelastic behavior of coating solutions.

[165] Pradhan, D. K., Choudhary, R. N. P., & Samantaray, B. K. (2008). Studies of dielectric relaxation and AC conductivity behavior of plasticized polymer nanocomposite electrolytes. *Int. J. Electrochem. Sci*, *3*(5), 597-608.

[166] Kimura, K., Yajima, M., & Tominaga, Y. (2016). A highly-concentrated poly (ethylene carbonate)-based electrolyte for all-solid-state Li battery working at room temperature. *Electrochemistry Communications*, *66*, 46-48.

[167] Zhao, J., Zhang, J., Hu, P., Ma, J., Wang, X., Yue, L., Cui, G. (2016). A sustainable and rigid-flexible coupling cellulose-supported poly (propylene carbonate) polymer electrolyte towards 5 V high voltage lithium batteries. *Electrochimica Acta*, *188*, 23-30.

[168] Chai, J., Liu, Z., Zhang, J., Sun, J., Tian, Z., Ji, Y., . Cui, G. (2017). A superior polymer electrolyte with rigid cyclic carbonate backbone for rechargeable lithium ion batteries. *ACS applied materials & interfaces*, *9*(21), 17897-17905.

[169] Ambika, C., Karuppasamy, K., Vikraman, D., Lee, J. Y., Regu, T., Raj, T. A. B., ... & Kim, H. S. (2018). Effect of dimethyl carbonate (DMC) on the electrochemical and cycling properties of solid polymer electrolytes (PVP-MSA) and its application for proton batteries. *Solid State Ionics*, *321*, 106-114.

[170] Rajeswari, N., Selvasekarapandian, S., Sanjeeviraja, C., Kawamura, J., & Bahadur, S. A. (2014). A study on polymer blend electrolyte based on PVA/PVP with proton salt. *Polymer bulletin*, *71*(5), 1061-1080.

[171] Vijay Kumar, V., Balaganesan, G., Lee, J. K. Y., Neisiany, R. E., Surendran, S., & Ramakrishna, S. (2019). A review of recent advances in nanoengineered polymer composites. *Polymers*, *11*(4), 644.

[172] Mohammed, L., Ansari, M. N., Pua, G., Jawaid, M., & Islam, M. S. (2015). A review on natural fiber reinforced polymer composite and its applications. *International Journal of Polymer Science*, *2015*.

[173] Sadasivuni, K. K., Cabibihan, J. J., Deshmukh, K., Goutham, S., Abubasha, M. K., Gogoi, J. P., ... & Rao, K. V. (2019). A review on porous polymer composite materials for multifunctional electronic applications. *Polymer-Plastics Technology and Materials*, *58*(12), 1253-1294.

[174] Chen, X., Yin, J., Alfonso, G. C., Pedemonte, E., Turturro, A., & Gattiglia, E. (1998). Thermodynamics of blends of poly (ethylene oxide) with poly (methyl methacrylate) and poly (vinyl acetate): prediction of miscibility based on Flory solution theory modified by Hamada. *Polymer*, *39*(20), 4929-4935.

[175] Zhao, N., Wu, F., Xing, Y., Qu, W., Chen, N., Shang, Y., Chen, R. (2019). Flexible Hydrogel Electrolyte with Superior Mechanical Properties Based on Poly (vinyl alcohol) and Bacterial Cellulose for the Solid-State Zinc–Air Batteries. *ACS applied materials & interfaces*, *11*(17), 15537-15542.

[176] Shahzad, S., Shah, A., Kowsari, E., Iftikhar, F. J., Nawab, A., Piro, B., ... & Zou, Y. (2019). Ionic Liquids as Environmentally Benign Electrolytes for High-Performance Supercapacitors. *Global Challenges*, *3*(1), 1800023.

[177] Hemalatha, R., Alagar, M., Selvasekarapandian, S., Sundaresan, B., Moniha, V., Boopathi, G., & Selvin, P. C. (2019). Preparation and characterization of proton-conducting polymer electrolyte based on PVA, amino acid proline, and NH 4 Cl and its applications to electrochemical devices. *Ionics*, *25*(1), 141-154.

[178] Bozkurt, A., Ise, M., Kreuer, K. D., Meyer, W. H., & Wegner, G. (1999). Proton-conducting polymer electrolytes based on phosphoric acid. *Solid State Ionics*, *125*(1-4), 225-233.

[179] Badr, S., Sheha, E., Bayomi, R. M., & El-Shaarawy, M. G. (2010). Structural and electrical properties of pure and H 2 SO 4 doped (PVA) 0.7 (NaI) 0.3 solid polymer electrolyte. *Ionics*, *16*(3), 269-275.

[180] Lee, D. J., Agostini, M., Park, J. W., Sun, Y. K., Hassoun, J., Scrosati, B. (2013). Progress in Lithium–Sulfur Batteries: The Effective Role of a Polysulfide-Added Electrolyte as Buffer to Prevent Cathode Dissolution. *ChemSusChem*, *6*(12), 2245-2248.

[181] Jovanovski, V., González-Pedro, V., Giménez, S., Azaceta, E., Cabañero, G., Grande, H., ... & Bisquert, J. (2011). A sulfide/polysulfide-based ionic liquid electrolyte for quantum dot-sensitized solar cells. *Journal of the American Chemical Society*, *133*(50), 20156-20159.

[182] Kumar, P. P., & Yashonath, S. (2006). Ionic conduction in the solid state. Journal of Chemical Sciences, 118(1), 135-154.

[183] Kasap, S. (2006). Springer handbook of electronic and photonic materials. Springer Science & Business Media.

[184] Tan, M. J., Li, B., Chee, P., Ge, X., Liu, Z., Zong, Y., & Loh, X. J. (2018). Acrylamide-derived freestanding polymer gel electrolyte for flexible metal-air batteries. *Journal of Power Sources*, *400*, 566-571.

[185] Santos, F., Tafur, J. P., Abad, J., & Romero, A. J. F. (2019). Structural modifications and ionic transport of PVA-KOH hydrogels applied in Zn/Air batteries. *Journal of Electroanalytical Chemistry*, *850*, 113380.

[186] Lewandowski, A., & Świderska-Mocek, A. (2009). Ionic liquids as electrolytes for Li-ion batteries—an overview of electrochemical studies. *Journal of Power Sources*, *194*(2), 601-609.

[187] Zhu, X., Yang, H., Cao, Y., & Ai, X. (2004). Preparation and electrochemical characterization of the alkaline polymer gel electrolyte polymerized from acrylic acid and KOH solution. *Electrochimica acta*, *49*(16), 2533-2539

[188] Wu, G. M., Lin, S. J., & Yang, C. C. (2006). Alkaline Zn-air and Al-air cells based on novel solid PVA/PAA polymer electrolyte membranes. *Journal of Membrane Science*, *280*(1-2), 802-808.

[189] Wu, G. M., Lin, S. J., & Yang, C. C. (2006). Preparation and characterization of PVA/PAA membranes for solid polymer electrolytes. *Journal of Membrane Science*, *275*(1-2), 127-133.

[190] Liu, Q., Wang, Y., Dai, L., & Yao, J. (2016). Scalable Fabrication of Nanoporous Carbon Fiber Films as Bifunctional Catalytic Electrodes for Flexible Zn-Air Batteries. *Advanced Materials*, *28*(15), 3000-3006.

[191] Meng, F., Zhong, H., Bao, D., Yan, J., & Zhang, X. (2016). In situ coupling of strung Co4N and intertwined N–C fibers toward free-standing bifunctional cathode for robust,

efficient, and flexible Zn–air batteries. *Journal of the American Chemical Society*, *138*(32), 10226-10231.

[192] Park, J., Park, M., Nam, G., Lee, J. S., & Cho, J. (2015). All-solid-state cable-type flexible zinc–air battery. *Advanced Materials*, *27*(8), 1396-1401.

[193] G. Merle, S.S. Hosseiny, M. Wessling, K. Nijmeijer, New cross-linked PVA based polymer electrolyte membranes for alkaline fuel cells, J. Membr. Sci. 409-410 (2012) 191–199

[194] Tan, M. J., Li, B., Chee, P., Ge, X., Liu, Z., Zong, Y., & Loh, X. J. (2018). Acrylamide-derived freestanding polymer gel electrolyte for flexible metal-air batteries. *Journal of Power Sources*, *400*, 566-571.

[195] Tran, T. N. T., Chung, H. J., & Ivey, D. G. (2019). A study of alkaline gel polymer electrolytes for rechargeable zinc–air batteries. *Electrochimica Acta*, *327*, 135021

[196] Xu, Y., Zhang, Y., Guo, Z., Ren, J., Wang, Y., & Peng, H. (2015). Flexible, Stretchable, and Rechargeable Fiber-Shaped Zinc–Air Battery Based on Cross-Stacked Carbon Nanotube Sheets. *Angewandte Chemie International Edition*, *54*(51), 15390-15394.

[197] Fan, X., Liu, J., Song, Z., Han, X., Deng, Y., Zhong, C., & Hu, W. (2019). Porous nanocomposite gel polymer electrolyte with high ionic conductivity and superior electrolyte retention capability for long-cycle-life flexible zinc–air batteries. *Nano energy*, *56*, 454-462.

[198] Fu, J., Lee, D. U., Hassan, F. M., Yang, L., Bai, Z., Park, M. G., & Chen, Z. (2015). Flexible High-Energy Polymer-Electrolyte-Based Rechargeable Zinc–Air Batteries. *Advanced materials*, *27*(37), 5617-5622.

[199] Xu, Y., Zhang, Y., Guo, Z., Ren, J., Wang, Y., & Peng, H. (2015). Flexible, Stretchable, and Rechargeable Fiber-Shaped Zinc–Air Battery Based on Cross-Stacked Carbon Nanotube Sheets. *Angewandte Chemie International Edition*, *54*(51), 15390-15394.

[200] Li, M., Liu, B., Fan, X., Liu, X., Liu, J., Ding, J., Zhong, C. (2019). Long-Shelf-Life Polymer Electrolyte Based on Tetraethylammonium Hydroxide for Flexible Zinc–Air Batteries. *ACS applied materials & interfaces*, *11*(32), 28909-28917.

[201] Bose, P., Deb, D., & Bhattacharya, S. (2019). Lithium-polymer battery with ionic liquid tethered nanoparticles incorporated P (VDF-HFP) nanocomposite gel polymer electrolyte. *Electrochimica Acta*, *319*, 753-765.

[202] Aziz, S. B., Woo, T. J., Kadir, M. F. Z., & Ahmed, H. M. (2018). A conceptual review on polymer electrolytes and ion transport models. *Journal of Science: Advanced Materials and Devices*, *3*(1), 1-17.

[203] Lewandowski, A., & Świderska-Mocek, A. (2009). Ionic liquids as electrolytes for Li-ion batteries—an overview of electrochemical studies. *Journal of Power Sources*, *194*(2), 601-609.

[204] Huie, M. M., DiLeo, R. A., Marschilok, A. C., Takeuchi, K. J., & Takeuchi, E. S. (2015). Ionic liquid hybrid electrolytes for lithium-ion batteries: a key role of the separator–electrolyte interface in battery electrochemistry. *ACS applied materials & interfaces*, *7*(22), 11724-11731.

[205] Galiński, M., Lewandowski, A., & Stępniak, I. (2006). Ionic liquids as electrolytes. *Electrochimica acta*, *51*(26), 5567-5580.

[206] Song, Y., Hu, J., Tang, J., Gu, W., He, L., & Ji, X. (2016). Real-time X-ray imaging reveals interfacial growth, suppression, and dissolution of zinc dendrites dependent on anions of ionic liquid additives for rechargeable battery applications. *ACS applied materials & interfaces*, *8*(46), 32031-32040.

[207] Kar, M., Winther-Jensen, B., Forsyth, M., & MacFarlane, D. R. (2013). Chelating ionic liquids for reversible zinc electrochemistry. *Physical Chemistry Chemical Physics*, *15*(19), 7191-7197.

[208] Kar, M., Ma, Z., Azofra, L. M., Chen, K., Forsyth, M., & MacFarlane, D. R. (2016). Ionic liquid electrolytes for reversible magnesium electrochemistry. *Chemical communications*, *52*(21), 4033-4036.

[209] Liu, Z., El Abedin, S. Z., & Endres, F. (2015). Dissolution of zinc oxide in a protic ionic liquid with the 1-methylimidazolium cation and electrodeposition of zinc from ZnO/ionic liquid and ZnO/ionic liquid–water mixtures. Electrochemistry Communications, 58, 46-50.

[210] Liu, Z., Pulletikurthi, G., Lahiri, A., Cui, T., & Endres, F. (2016). Suppressing the dendritic growth of zinc in an ionic liquid containing cationic and anionic zinc complexes for battery applications. Dalton Transactions, 45(19), 8089-8098.

[211] C. O. Laoire, S. Mukerjee, K. M. Abraham, E. J. Plichta and M. A. Hendrickson, J. Phys. *Chem. C*, 2009, 113, 20127

[212] Zhao, Y., Wan, J., Yao, H., Zhang, L., Lin, K., Wang, L., ... & Gu, L. (2018). Few-layer graphdiyne doped with sp-hybridized nitrogen atoms at acetylenic sites for oxygen reduction electrocatalysis. Nature chemistry, 10(9), 924-931.

[213] Kar, M., Simons, T. J., Forsyth, M., & MacFarlane, D. R. (2014). Ionic liquid electrolytes as a platform for rechargeable metal–air batteries: a perspective. Physical chemistry chemical physics, 16(35), 18658-18674.

[214]Kartha, T. R., & Mallik, B. S. (2020). Ionic conductance and viscous drag in water-in-salt electrolytes for lithium and sodium ion batteries and supercapacitors. Materials Today Communications, 101588.

[215] UMD/USARL team develops "water-in-salt" electrolyte enabling high-voltage aqueous Li-ion chemistries , https://www.greencarcongress.com/2015/11/umdusarl-team-develops-water-in-salt-electrolyte-enabling-high-voltage-aqueous-li-ion-chemistries.html

[216] Wang, F., Borodin, O., Gao, T., Fan, X., Sun, W., Han, F., ... & Wang, C. (2018). Highly reversible zinc metal anode for aqueous batteries. Nature materials, 17(6), 543-549.

[217] De, S., White, J., Brusuelas, T., Patton, C., Koh, A., & Huang, Q. (2020). Electrochemical behavior of protons and cupric ions in water in salt electrolytes with alkaline metal chloride. Electrochimica Acta, 338, 135852.

[218]Chen, M., Feng, G., & Qiao, R. (2020). Water-in-salt electrolytes: An interfacial perspective. Current Opinion in Colloid & Interface Science, 47, 99-110.